Coupled survey of lithium isotopes and Li/Ca in biogenic and inorganic carbonates

Dongyu Chen, Fanny Thibon, Axel Felbacq, Lucas Weppe, Marc Metian, Nathalie Vigier

Coupled survey of lithium isotopes and Li/Ca in biogenic and inorganic carbonates

Dongyu Chen[a*], Fanny Thibon[a], Axel Felbacq[a], Lucas Weppe[a], Marc Metian[b], Nathalie Vigier[a]

[a] Laboratoire d'Océanographie de Villefranche (LOV), UMR 7093, CNRS, Sorbonne université, 06230 Villefranche-sur-Mer, France

[b] International Atomic Energy Agency (IAEA), Marine Environment Laboratories, Radioecology laboratory, 4a, Quai Antoine Ier, MC-98000 Principality of Monaco, Monaco

*corresponding author

Abstract

Geochemists have long considered Li isotope composition of marine carbonates as one of the most straightforward oceanic archives, tracing climate regulation by continental silicate weathering. However, despite an isotopically homogenous ocean, a large range of δ^7Li values were reported in the literature for modern biogenic carbonates. Additionally, laboratory studies highlighted variable Li isotope fractionations during foraminifera growth and during precipitation of inorganic carbonates.

Despite an increasing interest in this topic, there is still limited understanding of Li isotopic fractionation and of Li incorporation mechanisms in carbonates. The present review aims to filling this gap by compiling and meta-analyzing the past findings from the literature. More specifically, Li/Ca and δ^7Li data concerning the influence of mineralogy, temperature, pH, growth rate and biological processes have been exhaustively reviewed and statistically examined, including by PCA (Principal Component Analysis). For inorganic carbonate, we demonstrate that (1) the influence of mineral type is insufficiently explored (2) the effect of temperature on Li isotopes is negligible, although temperature changes can affect calcite Li/Ca ratio, and (3) calcite δ^7Li and Li/Ca are primarily influenced by pH and growth rate. For marine modern biogenic carbonates, our cartography highlights an uneven geographical distribution, and further studies are required in the Pacific, Indian, and Southern Oceans. Also, for both Li/Ca and δ^7Li, there are statistically significant and systematic differences between 'bulk carbonates' and all studied marine biogenic groups (i.e. foraminifera, mollusks, brachiopods). A detailed examination of foraminifera data reveals that planktic species display δ^7Li values statistically higher than benthic ones, and both anti-correlate with Li/Mg ratios. Overall, this review underlines the necessity of filling the identified gaps of knowledge and of attentively considering the impact of environmental parameters and biological processes for interpreting past δ^7Li variations displayed by fossil shells.

Keywords: lithium isotopes, Li/Ca, marine carbonates, vital effects, synthesis

1. Introduction

Lithium (Li) is the least dense of all metals and naturally occurs in the environment as a free Li^+ ion surrounded by water molecules (Olsher et al., 1991). During the formation of carbonates in the ocean, Li can be incorporated as a trace element in their crystallographic structure and its Li isotopic composition has been used to reconstruct the ocean Li isotope variations for inferring the relationship between climate, pCO_2 (partial pressure of carbon dioxide), and continental silicate weathering (Hathorne and James, 2006; Kalderon-Asael et al., 2021; Misra and Froelich, 2012). Indeed, Li is composed of two stable isotopes, ^6Li and ^7Li, representing 7.59% and 92.41%, respectively, with a high ability to fractionate. The Li isotopic variations observed on earth display the second largest range among non-conventional isotopes, with values exceeding 40‰ (Li isotopic composition being reported as $\delta^7Li = ([(^7Li/^6Li)/(^7Li/^6Li)_{L\text{-}SVEC} - 1] \times 1000$, L-SVEC being the international standard provided by the US National Institute of Standards and Technology).

Modern oceans contain approximately 230 billion tons of Li. Their primary sources of Li are rivers and high-temperature hydrothermal fluids, which have modern fluxes of similar magnitude, of about 10×10^9 and 13×10^9 mol $year^{-1}$, respectively (Misra and Froelich, 2012). The average δ^7Li value of modern river waters is 23‰, with a range from 2‰ to 43‰ (Dellinger et al., 2015; Huh et al., 1998), which is higher than for marine hydrothermal fluids (8.3‰) (Chan et al., 1993; Chan et al., 1994). Owing to the large oceanic residence time of Li (~1.5 million year) (Huh et al., 1998), Li concentration and isotopic composition of seawater

are spatially homogeneously distributed ($[Li]_{SW}$ ~ 26 μM; δ^7Li_{SW} = 31 ± 0.3‰) in the modern ocean (Millot et al., 2004), except close to hydrothermal sites (Artigue et al., 2022).

During weathering of silicate rocks (e.g., incongruent continental weathering, off-axis seafloor alteration, and reverse weathering in marine sediments), ^6Li is preferentially incorporated into secondary minerals, leaving residual waters enriched in ^7Li (Chan et al., 1992; Huh et al., 1998; Pistiner and Henderson, 2003). As a result, past variations in seawater δ^7Li have primarily been attributed to changes in global weathering regimes in response to climate or tectonic events (Crockford et al., 2020; Hathorne and James, 2006; Kalderon-Asael et al., 2021; Lechler et al., 2015; Misra and Froelich, 2012; Pogge Von Strandmann et al., 2013; Sun et al., 2018).

Systematically, oceanic water δ^7Li value is frequently assumed to be similar to the carbonate record. However, determining if the formation of biogenic carbonates in the ocean is related to significant and variable Li isotope fractionations remains challenging. Low Li concentrations in these mineral phases, effects of diagenesis, and potential contamination from Li-rich authigenic minerals may bias their pristine isotopic signatures (Bastian et al., 2018; Dellinger et al., 2020; Pogge Von Strandmann et al., 2019). It was not until the late 20th century that scientists first analyzed four samples of Pleistocene foraminifera *Pulleniatina obliquiloculata* as well as two marine carbonates by thermal ionization mass spectrometry (TIMS) (You and Chan, 1996). Their results showed that foraminifera have lighter Li isotopic composition (19.3‰, 23.0‰) during glacial times, compared to interglacial (26.6‰, 42.2‰). Then, Hoefs and Sywall. (1997) found a large fluctuation (from 7‰ to 20‰) for

mixed planktic species through the Holocene, partly attributed to inadequate sample cleaning. Kosler et al. (2001) measured δ^7Li in core-top *Pulleniatina obliquiloculata* by Quadrupole Inductively Coupled Plasma Mass Spectrometry (ICP-MS) and reported δ^7Li values from 27.9‰ to 31.3‰ (modern seawater value being 31.2‰ ± 0.3‰).

In the past, the determination of Li isotope compositions in marine carbonates was constrained by instrumentation with low precision, typically exceeded 2‰. More recently, the precision was improved (Table S1), For instance, Li isotopes have been measured in low level marine carbonates using Q-ICP-MS associated to a desolvating system, within ±1.6 ‰ (2σ) in precision (Misra and Froelich, 2009; Seyedali et al., 2021, Vigier et al., 2008). The use of SIMS (Secondary Ion Mass Spectrometry / ion microprobe) also enables (*in situ*) δ^7Li analyses for carbonate minerals, while avoiding contamination from surface Fe-oxydes and clays, with a reproducibility of 1.5‰ - 2‰ (2σ) (e.g. Vigier et al., 2007; Rollion-Bard et al., 2009). More recently, Multicollector-Inductively Coupled Plasma Mass Spectrometer (MC-ICP-MS) have allowed to achieved the measurement of Li isotopes in multiple carbonates samples, with a precision of about 0.5‰-0.8‰ (2σ) (e.g. Dellinger et al., 2020; Pogge von Strandmann et al., 2019). As a result, numerous δ^7Li values have been published for various groups (e.g. foraminifera (Bastian et al., 2018; Hathorne and James, 2006; Roberts et al., 2018; Vigier et al., 2015; Vigier et al., 2007), corals (Bastian et al., 2018; Dellinger et al., 2018; Marriott et al., 2004; Rollion-Bard et al., 2009), mollusks (Dellinger et al., 2018), echinoderms (Dellinger et al., 2018), brachiopods (Dellinger et al., 2018; Gaspers et al., 2021; Washington et al., 2020)), as well as for marine bulk carbonate extracted by

sediment leaching (e.g. Dellinger et al., 2020; Murphy et al., 2022; Pogge Von Strandmann et al., 2019).

Cultures of calcifying species have been performed under controlled conditions (e.g. foraminifera (Roberts et al., 2018; Vigier et al., 2015) brachiopods (Gaspers et al., 2021), and mollusks (Dellinger et al., 2018)). Also, inorganic carbonate phases have been grown at the laboratory to study inorganic Li isotope fractionations ($\Delta^7Li_{carb\text{-}sol}$) and their controls, which were compared to their biogenic equivalent (Day et al., 2021; Füger et al., 2022; Gabitov et al., 2011; Marriott et al., 2004; Marriott et al., 2004; Seyedali et al., 2021; Taylor et al., 2019).

Table 1: Summary of the Li isotopic composition of biogenic and abiogenic carbonates.

	$\Delta^7Li_{carb\text{-}sol}$ Minimum	$\Delta^7Li_{carb\text{-}sol}$ Maximum	Mean	2sd	N
Biogenic calcite	-11.5‰	+9.7‰	-2.83‰	6.5	192
Synthetic calcite	-10.1‰	+3.8‰	-5.11‰	6.1	73
Biogenic aragonite	-16.2‰	-5.7‰	-11.7‰	4.2	168
Synthetic aragonite	-12.0‰	-7.7‰	-10.9‰	2.9	8

References for biogenic calcite are from (Marriott et al., 2004a; Hall et al., 2005; Hathorne and James, 2006; Vigier et al., 2007; Misra and Froelich, 2012; Vigier et al., 2015; Dellinger et al., 2018; Roberts et al., 2018; Washington et al., 2020; Gaspers et al., 2021; Hall and Chan, 2004; Bryan and Marchitto, 2008; Yun et al., 2005; Bryan and Marchitto, 2008; Hendry et al., 2009; Delaney et al., 1989) ; synthetic calcite are from : (Day et al., 2021; Marriott et al., 2004a; Marriott et al., 2004b; Füger et al., 2022; Seyedali et al., 2021; Gabitov et al., 2011; Füger et al., 2022); for biogenic aragonite from: (Marriott et al., 2004b; Rollion-Bard et al., 2009; Bastian et al., 2018; Dellinger et al., 2018; Cuny-Guirriec et al., 2019; Dellinger et al., 2020), and for synthetic aragonite from: (Day et al., 2021; Gabitov et al., 2011; Marriott et al., 2004;).

In the last 5-10 years, as the study of marine carbonates intensified, researchers have gradually found that modern marine carbonates exhibit a significant range of Li isotopic compositions (Table 1 and Fig. 1). The isotopic fractionation $\Delta^7Li_{carb\text{-}sol}$ can vary from -16.2‰

(Aragonite mussel (Dellinger et al., 2018)) to +9.7‰ (Calcite scallop (Dellinger et al., 2018)).

Theoretically, "vital effects" can be quantified when comparing the isotope signature of biogenic and inorganic phases (Dellinger et al., 2018; Pogge Von Strandmann et al., 2019). However, when we compile all published data from the literature, it appears that the range of $\Delta^{7}Li_{carb\text{-}sol}$ values in inorganic phases is as large as that of biogenic phases (see Fig. 1). Consequently, it is difficult to use this method to demonstrate either the lack or the occurrence of biological Li isotope fractionations. Another key point is that the Li concentrations (or Li/Ca ratios) are rarely discussed while the environmental controls of biogenic Li concentrations may also impact Li isotopes (Thibon et al., 2021).

The present study compiles, to the best of our knowledge, all the published data on modern carbonates. Due to the low Li levels in modern marine carbonate, their Li concentration and isotopic compositions are easily influenced by silicate minerals present in the same environment (clay micrograins in particular) (Pogge Von Strandmann et al., 2021; Dellinger et al., 2020; Pogge Von Strandmann et al., 2019; Bastian et al., 2018; Dellinger et al., 2018; Misra and Froelich, 2009; Vigier et al., 2007; Hall et al., 2005). As a consequence, our dataset does not include carbonates that have been affected by marine diagenesis. Since different authors may have inconsistent criteria for diagenetic imprint (e.g., Mn/Ca, Al/Ca, Sr/Fe, Li/(Mg+Ca), etc.), and there are significant differences in the criteria for assessing contamination in carbonate samples coming from different sites and sedimentary contexts, we strictly followed each authors' standards when selecting data to include.

Through statistical tests, we aim to clarify the potential differences in Li isotopic compositions and in Li/Ca among the various carbonate phases, and various categories, but also evaluate the role of environmental parameters when possible. This work also tentatively highlights the gaps to fill for future works in paleo-environment and paleoceanography.

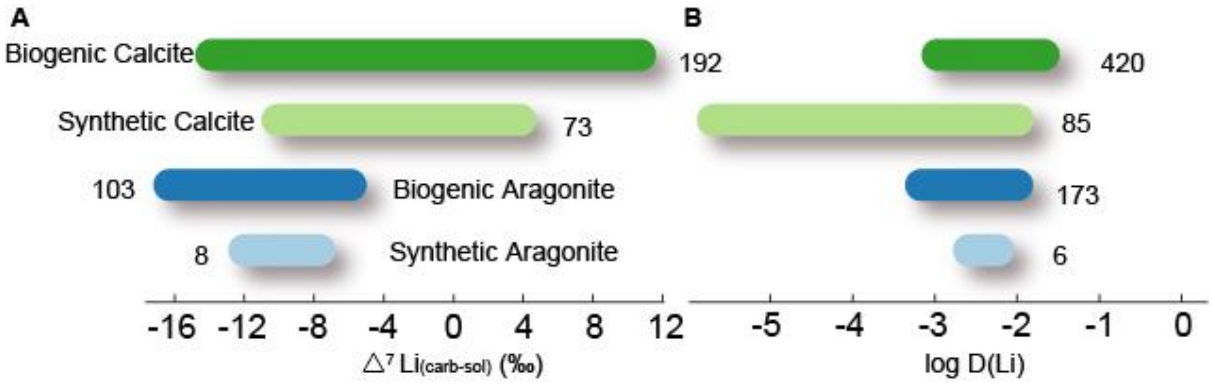

Fig. 1: Range of **A)** carbonate - water Li isotope fractionations ($\Delta^7Li_{carb\text{-}sol}$) and **B)** Li partition coefficients (D(Li) in µmol mol^{-1} = $(Li/Ca)_{carb}/(Li/Ca)_{sol}$) published for inorganic calcite (light green), inorganic aragonite (light blue), modern biogenic calcite (dark green) and modern biogenic aragonite (dark blue). Modern biogenic phases include core-top data and a few living organisms. More detailed subset data can be found in the Sup. Mat. Table S2. Same references as in Table 1.

2. Multiple controls of Li/Ca and Li isotopes during inorganic carbonate growth

To date, seven studies investigated the Li isotopic composition of synthetic carbonates grown under controlled conditions (Day et al., 2021; Füger et al., 2022; Gabitov et al., 2011; Marriott et al., 2004; Marriott et al., 2004; Seyedali et al., 2021; Taylor et al., 2019). While the study conducted by Taylor et al. (2019) focuses on carbonate formation at high temperatures (which is not discussed here), the remaining studies utilized a wide range of

171 experimental conditions, as summarized in Table 2.

172 Marriott et al. (2004a) were the pioneers in investigating the effect of temperature on the Li
173 isotopic composition of inorganic carbonates. At different temperatures (5-30°C), calcite is
174 synthesized by mixing $CaCl_2$ and $NaHCO_3$ solutions. The authors report a Li isotopic
175 fractionation $\Delta^7Li_{carb\text{-}sol} \sim -8‰$, unaffected by temperature. In contrast, calcite Li/Ca ratio
176 decreases significantly with increasing temperature (from 7.51 to 2.47 μmol mol^{-1}). Marriott
177 et al. (2004b) further investigated the influences of minerals and salinity. Their results show
178 that the mineral type has a decisive effect on Li isotopes. Indeed, the Li isotope fractionation
179 during aragonite growth is relatively large (-11‰) compared to the calcite one (-3‰).
180 Salinity variations (from 10 to 50 psu) do not affect the Li isotopic composition for both
181 minerals. Nevertheless, an increase in solution salinity increases the Li/Ca ratio of calcite
182 (from 14.5 to 62.9 μmol mol^{-1}), while aragonite Li/Ca remains essentially constant (19.3
183 μmol mol^{-1}). Importantly, a comparison of the two studies (Marriott et al., 2004a and 2004b)
184 reveals a significant difference in the Li isotopic fractionation during calcite formation (of
185 5‰). One potential explanation might be the higher solution pH used in Marriott et al.
186 (2004b) compared to Marriott et al. (2004a) (pH= 7.7 to 8.3 vs. 6.9 to 7.1, respectively).
187 Another factor could be that Marriott et al. (2004b) precipitated calcite from artificial
188 seawater, while Marriott et al. (2004a) used deionized water.

189 Several years later, Gabitov et al. (2011) precipitated aragonite by adding Na_2CO_3 to
190 pre-concentrated seawater (1L of seawater was evaporated to half of its volume). The
191 corresponding $\Delta^7Li_{carb\text{-}sol}$ ranges from -10.5‰ to -7.7‰, which is smaller in magnitude

compared to the findings of Marriott et al. (2004b) (-11‰). In 2021, Day et al. simulated cave stalagmites precipitation by degassing. They dropped a calcite-saturated solution from a container with a high partial pressure of carbon dioxide, into a container with a lower partial pressure of carbon dioxide. The initial solution was made from dissolved calcite spiked with trace elements. The Li isotope fractionation $\Delta^7Li_{carb\text{-}sol}$ is -6.5 to -9.9‰ for calcite, -7.3 ± 0.6‰ for high-Mg calcite (HMC), and -10.7 ± 0.5‰ for aragonite. In contrast to Marriott et al. (2004b), the study indicates that carbonate minerals have a limited influence Li isotopic fractionation. Instead, they highlight a strong influence of the mineral growth rate, with higher rates leading to larger Li isotopic fractionation.

The same year, Seyedali et al. (2021) grew calcite under controlled conditions by mixing $CaCl_2$ and $NaHCO_3$ solutions at different pH. They find that the $\Delta^7Li_{carb\text{-}sol}$ values increase from -6‰ to +2‰ as the pH increase. They suggest a key role of Li speciation inferring that Li in solution is first bound into calcite as $LiHCO_3$ before being incorporated into the calcite structure. Thus, their $\Delta^7Li_{carb\text{-}sol}$ values may result from kinetics processes related to surface attachment and from changes in the Li speciation in solution, depending on both dissolved carbon concentration and pH.

Most recently, by mixing $CaCl_2$ and $NaHCO_3$ solutions to grow calcite grains, Füger et al. (2022) find that the $\Delta^7Li_{carb\text{-}sol}$ values range from -5.3‰ to -1.8‰, and decrease in magnitude when solution pH increases (under a growth rate of $10^{-7.5}$ to $10^{-7.9}$ mol m^{-2} s^{-1}), or when the growth rate decreases (for $8.1 < pH < 8.4$).

Overall, most experiments led to a lighter Li isotopic composition of the synthesized carbonates relative to the growth solution, except for a few data published by Seyedali et al. (2021). Additionally, all experiments led to significantly low D(Li) ($< 10^{-1} – 10^{-5}$), essentially expressing the lack of compatibility of Li into carbonate phases. In the following, we further detail the current knowledge on major control factors investigated in the literature (mineralogy, temperature, pH, growth rate).

Table 2: Summary of the characteristics of all published experiments of inorganic carbonate precipitation. *HMC indicates high magnesium calcite.

	Marriott et al. 2004a	Seyedali et al. 2021	Day et al. 2021	Fuger et al. 2022	Marriott et al. 2004b	Gabitov et al. 2019	Day et al. 2021	Marriott et al. 2004b	Gabitov et al. 2011	Day et al. 2021
Mineralogy	Calcite	Calcite	Calcite	Calcite	Calcite	Calcite	Aragonite	Aragonite	Aragonite	*HMC
Seed crystal	Calcite	Vaterite	Calcite	Calcite	Calcite	Unseeded	Calcite	Calcite	Unseeded	Calcite
Media solution	Deionized water	Deionized water	Deionized water	NaCl solution	Artificial seawater	Artificial seawater	Deionized water	Artificial seawater	Natural Seawater	Deionized water
Li source	LiCl	Li_2CO_3	-	LiCl	Li_2CO_3	Na_2CO_3	-	Li_2CO_3	Li_2CO_3	-
Reactants	$CaCl_2$ $NaHCO_3$	$CaCl_2$ Na_2CO_3	$Ca(HCO_3)_2$	$CaCl_2$ Na_2CO_3	$CaCl_2$ Na_2CO_3		$Ca(HCO_3)_2$	$CaCl_2$ Na_2CO_3	Na_2CO_3	$Ca(HCO_3)_2$
Li (µmol L^{-1})	176 to 210	90 to 570	25 to 71	230 to 500	82 to 409	44.5 and 47.4	17	82 to 409	~ 600	28
Mg (mmol L^{-1})	0	0	0.044 to 0.14	0	1.5 to 7.6	42.4 and 42.5	4.7	15 to 76	1.22	2.5
Ca (mmol L^{-1})	240 to 470	0.02 to 135.93	2.0 to 4.8	0.1 to 12.17	2.85 to 14.3	7.3and 7.6	1.2	2.85 to 14.3	229.54	1.9
pH	6.9 to 7.1	6.2 to 9.5	7.4 to 8.1	6.31 to 9.59	7.7 to 8.3	8.55 and 8.54	8.3	7.7 to 8.3	-	8.1
T (°C)	5 to 30	20.7±1.5	7 to 35	25	25	24	20	25	25	20
Duration (days)	0.21	5 to 400	21	1	0.33	244	21	0.33	-	21

2.1 Debated mineralogical control

Synthetic inorganic carbonates include three types: calcite, aragonite, and high-magnesium calcite (HMC). As illustrated in Fig. 1, most published Li/Ca and δ^7Li values concern calcite minerals (n = 85 and 73 respectively), while there are only few experimental data for inorganic aragonite (n = 6 and 8 respectively). Therefore, it remains difficult to compare both datasets statistically. For inorganic calcite, every additional published experiment has enlarged the range of values for $\Delta^7Li_{carb\text{-}sol}$ and D(Li), and we can suspect that it will be the same for experimental aragonite in the future.

Another concern arises from the lack of synthesis experiments conducted under natural seawater conditions. Although Gabitov et al. (2011) initially employed seawater, they diminished its volume by half through evaporation. Consequently, the concentrations of all dissolved elements were twice as high as those found in typical natural seawater. Other published experiments used simplified artificial seawater or deionized water.

In a seawater-like (synthetic) environment (Gabitov et al., 2011; Marriott et al., 2004), the Li isotope fractionation during calcite growth (-3.1‰ to -1.9‰) is smaller compared to one obtained during aragonite growth (-7.7‰ to -12‰). A similar phenomenon can be observed when deionized water is used; however, the extent of fractionation displayed by calcite synthesized in deionized water can be greater (-10.1‰ to +0.2‰) (Day et al., 2021; Füger et al., 2022; Marriott et al., 2004). Yet, more data

241 are required for a reliable statistical treatment and establish the role of the solution
242 chemical composition.
243 Concerning carbonate Li contents, we can compare different contexts and
244 experiments by using Li partition coefficients ($D(Li) = (Li/Ca)_{calcite} / (Li/Ca)_{solution}$).
245 For inorganic calcite, D(Li) range is wider than for inorganic aragonite ($10^{-5.7}$ - 10^{-2}
246 and $10^{-2.6}$ - $10^{-2.2}$, respectively), but the number of data is scarce for the latter (Fig. 1).
247 For HMC there is currently only one data ($10^{-1.9}$).
248 Given that Li ions are incorporated differently into the calcite and the aragonite
249 structures, a significant discrepancy between both phases would be expected for both
250 Li isotopes and D(Li). Indeed, Li ions substitute for the Ca ions site in aragonite,
251 whereas in calcite, Li can be incorporated into interstitial positions in its hydrated
252 form (Marriott et al., 2004a). This may explain why calcite D(Li) increases with
253 increasing salinity, while aragonite D(Li) remains relatively stable when salinity
254 varies (Marriott et al., 2004a). More data are however needed to better quantify these
255 aspects, particularly for aragonite and HMC.

256 ## 2.2 Small influence of temperature

257 Two studies found that the Li isotope fractionation between calcite and growth
258 solution ($\Delta^7Li_{carb\text{-}sol}$) is negligibly affected by temperature (Day et al., 2021; Marriott
259 et al., 2004a). Day et al. (2021) experiment led to a slight but significantly negative
260 correlation with temperature, as shown in Fig. 2A. In their experiment, other

parameters such as pH and growth rate (see Fig. 2C, 2E) varied as well, and among them it appears that temperature induced the smallest effect.

In contrast, D(Li) (expressed as logD(Li)) corresponding to synthetic calcites show a very consistent and negative correlation with temperature (R = -0.94, Day et al., 2021; Marriott et al., 2004a). Thus, calcite formed at high temperatures contains less Li than at low temperatures (Fig. 2B). Both studies give consistent results and used a Ca solution enriched in Li as the growth medium, although the technique used to reach saturation was different (see Table 1). Interestingly, two other experimental studies of inorganic calcite formation (Füger et al., 2022; Seyedali et al., 2021), show that, at constant temperature, the variations in both Li isotope values and D(Li) values are much larger than those caused by varying the temperature alone. It strongly suggests that temperature is not the dominant control factor and that other parameters play a crucial role in Li incorporation by calcite.

Finally, Day et al. (2021) and Marriott et al. (2004a) evaluate the effect of temperature for aragonite and high magnesium calcite. Their Li data are roughly consistent with the results obtained for calcite. Nevertheless, additional experiments, covering a larger temperature range, are required to precisely confirm these statements (see Fig. 2A and 2B).

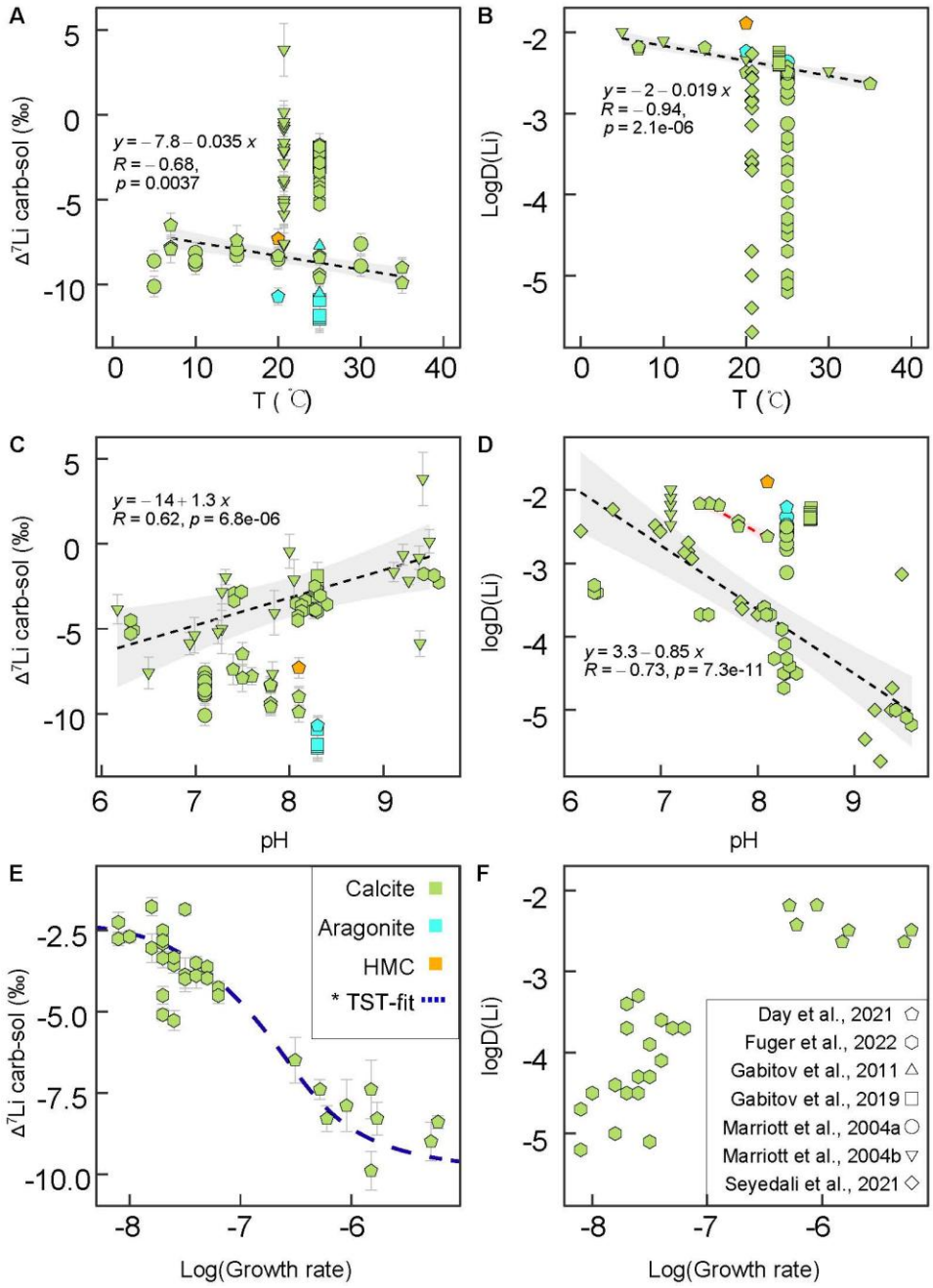

Fig. 2: Compilation of Li isotopic fractionations and Li partition coefficients between precipitated inorganic carbonate and growth solution. Each data point represents a value measured for one carbonate aliquot **(A and B)** Effect of temperature. The black dashed lines indicate linear regressions for calcite, gray shading represents confidence intervals. Data are from Marriott et al. (2004a) and Day et al. (2021); **(C and D)** Effect of the solution (final) pH. Black dashed lines indicate linear regressions for calcite. Data are from Seyedali et al. (2021) and Füger et al. (2022); **(E and F)** Effect of the growth rate (in log10). The trend shown in Fig. 2E is reported from Fuger et al. (2022) and represents a TST model using specific modifications (e.g. backward calcite dissolution rate), distinguishing it from the TST model classically used for divalent ions (see text for more details).

2.3 Significant influence of pH

Fig. 2C reveals a strong linear relationship between Li isotope fractionation for calcite and the solution pH. As the pH decreases, the extent of fractionation increases. Similarly, for calcite, there is a significant linear relationship between the logD(Li) and pH, where lower pH values correspond to higher logD(Li) values and (Fig. 2D). The observed similarity in the behavior of Li isotope fractionation and elemental partitioning in calcite with respect to pH suggests the involvement of a common mechanism regulating both processes.

There is still controversy regarding the species in which Li is incorporated into forming carbonate, and if the solution pH may play a role. Some authors argue that there is only one type of Li incorporated into calcite, while others propose that there are more than two Li species, depending on the pH. For example, Seyedali et al. (2021) suggested that over a large pH range (between 6.2 and 9.5), the most likely form of Li incorporation into calcite is as $LiHCO_3$ (rather than as Li_2CO_3 or $LiNaCO_{3)}$. The authors argue that in the absence of kinetic effects and with constant activity coefficients, the overall process of Li incorporation into calcite must maintain charge balance. Therefore, the equilibrium constants for the $LiHCO_3$ should remain unchanged as a function of pH (for a given growth rate). Fuger et al. (2019, 2022). propose that the dominant reaction for Li incorporation into calcite is as follows:

$$Li^{+}_{(aq)} + H^{+}_{(aq)} + CaCO_{3\,(s)} \leftrightharpoons LiHCO_{3\,(s)} + Ca^{2+}_{(aq)},$$

which indicates that Li incorporation in calcite is not only related to the solution HCO_3^-, but also controlled by the Li^+ and Ca^{2+} concentration of the solution. When the dissolved concentration of Ca^{2+} and Li^+ are constant (e.g. Ca^{2+}saturated solution), a decrease in pH triggers $LiHCO_3$ formation, and more Li can be incorporated into calcite. In contrast, when dissolved Ca concentration is not constant (the Ca^{2+} concentration is usually increased at lower pH to keep an oversaturated medium), a lower pH results in less $LiHCO_3$ formation and, therefore, in less Li in calcite. This may explain why we observe a negative correlation between logD(Li) and pH in Fig. 2D. Fuger et al. (2022) therefore suggest that $LiHCO_3$ is dominant within a specific pH range, rather than the entire range of 6.3 to 9.5.

Concerning Li isotopes, early precipitation experiments (Marriott et al., 2004a; Marriott et al., 2004b) did not consider pH as a potential variable because Li^+ in seawater mainly remains surrounded by four water molecules, in contrast with other biogeochemical tracers such as boron, for which speciation in seawater is known to be pH dependent (e.g. Foster and Rae, 2016). Nevertheless, a positive correlation was recently found for inorganic calcite between $\Delta^7Li_{carb\text{-}sol}$ and solution pH (Seyedali et al., 2021; Füger et al., 2019; Marriott et al., 2004a; Marriott et al., 2004b). As the pH of the solution increases, the extent of fractionation of the calcite Li isotope decreases. As shown in Fig. 2C, this pH effect may reconcile the isotopic discrepancy observed between the two Marriott et al. studies (2004a; 2004b). In contrast, the stalactite experiments performed by Day et al. (2021) exhibit a small (negative) correlation between $\Delta^7Li_{carb\text{-}sol}$ and solution pH, but the range of tested pH was narrow (from 7.4

to 8.3 Fig. 2C), and the calcite growth rate significantly higher. It cannot be excluded that variations in the Li aqueous speciation caused by changes in solution chemistry may induce changes in the equilibrium isotopic fractionation factor. Indeed, under a given growth rate and at isotopic equilibrium, if dissolved Li occurs under as a single specie only, the isotopic fractionation should remain constant.

Another parameter of importance is the Saturation Index (SI), which is often related to the solution pH. In our Fig. S2 (Supplementary Material), we can see that at a single SI, a large variation of isotopic fractionations can be found. Also, when SI increases significantly, relatively small $\Delta^{7}Li_{carb\text{-}sol}$ variations are observed. This preliminary observation suggests a weak influence of the SI on Li isotopic fractionation. However, as experimental conditions among the various studies are very distinct in salinity, in solution chemical composition and in calcium concentrations, it is difficult to directly compare their SI values. More experimental work will need to be undertaken under natural seawater conditions to better evaluate the role of this parameter. Finally, it cannot be excluded that the trends as a function of pH (Fig. 2C and Fig. 2D) may also be – at least partly - driven by growth rates.

2.4 Strong influence of growth rate

Currently, there are two articles investigating the influence of the growth rate of inorganic calcite on Li isotope fractionation (Day et al., 2021; Füger et al., 2022). However, their measurement methods for growth rate differ. Füger et al. (2022) used mass balance equations. Day et al. (2021) applied image analysis to estimate the

surface area of calcite and conducted eight experiments to establish a relationship between surface area and growth mass. Despite these differences, the two studies display a consistent trend, as displayed in Fig. 2E and 2F and consequently we consider in the following that their comparison appears overall reasonable.

Füger et al. (2022) show that logD(Li) values of inorganic calcite increase with the calcite growth rate (usually expressed in mol m^{-2} s^{-1}) (Fig. 2F). As growth rates increase from $10^{-8.1}$ to $10^{-7.1}$ mol m^{-2} s^{-1}, D(Li) values rise strongly from $10^{-4.8}$ to $10^{-2.9}$, indicating that at a higher growth rate it is easier for Li to enter calcite grains. This was previously reported for divalent ions in calcite, i.e., Ba^{2+}, Sr^{2+}, Mg^{2+} (Gabitov and Watson, 2006; Mavromatis et al., 2018; Mavromatis et al., 2013). A growth entrapment model (GEM) was developed to explain this process (Watson, 2004). The GEM suggests that the surface composition of a crystal in equilibrium with a solution is usually different from that of a bulk crystal (as divalent ions are enriched at the crystal surface). If the crystal grows excessively fast, this equilibrium is broken, and the slower diffusing divalent ions become trapped and eventually form a solid by direct substitution of Ca ions.

However, Li^{+} ions do not usually directly replace Ca^{2+}, due to a large difference in ionic radii, and to charge imbalance (Füger et al., 2019). This behavior is expected to be close to that of Na and other alkali elements. Notably, it has been shown that Na^{+} concentration of calcite depends on the number of calcite defects (Busenberg and Niel Plummer, 1985). These crystal defects are controlled by the growth rate, i.e., the faster the growth rate, the more defects are observed at the surface of the newly

375 formed crystals, and the more Na^+ ions can enter the crystals. Okumura and Kitano.
376 (1986) reached the same conclusion for other alkali elements (K^+ and Rb^+). A recent
377 study further supported that D(Li) and D(Na) display a similar linear relationship with
378 growth rate (Füger et al., 2019). Overall, these studies indicate that growth rate plays
379 an essential role in the Li - and other alkali - content of calcite.
380 It is however noteworthy that no correlation between growth rate and logD(Li) was
381 observed in the slowly growing calcite from a doubly concentrated seawater solution
382 (Gabitov et al., 2019). It may be explained by the fact that natural seawater contains a
383 large amount of Mg^{2+} and SO_4^{2-}, which can readily incorporate the calcite and
384 potentially change its crystal structure. This discrepancy suggests that a direct
385 comparison of synthetic calcite with marine authigenic calcite is not always
386 appropriate, at least for D(Li).
387 Considering Li isotopes, the recent study of (Füger et al., 2022) revealed that calcite
388 $\Delta^7Li_{carb\text{-}sol}$ value remains essentially constant ($\Delta^7Li_{carb\text{-}sol}$ =-2.76±0.22‰) when the
389 calcite growth rate remains at a low level (< $10^{-7.7}$ mol m^{-2} s^{-1}). However, as the
390 growth rate increases (>$10^{-7.7}$ mol m^{-2} s^{-1}), the $\Delta^7Li_{carb\text{-}sol}$ increases rapidly in
391 magnitude. This indicates that more ^6Li is incorporated into calcite at higher growth
392 rates (Fig. 2E). Day et al. (2021) also observed a negative correlation between
393 $\Delta^7Li_{carb\text{-}sol}$ and growth rate (Fig. 2E). By comparing the data from Marriott et al.
394 (2004a) and Marriott et al., (2004b), although the surface area is not specified we note
395 that calcite with faster growth rates (0.2 g h^{-1} vs 0.09 g h^{-1}) leads to a larger isotopic

fractionation (-8‰ versus -3‰), , as initially suggested by (Day et al., 2021), and this is fully consistent with the above findings

Füger et al. (2022) suggested that, when the growth rate is slow, isotopic fractionation operates near equilibrium, the net reaction rates of precipitation and dissolution are essentially equal, $\Delta^{7}Li_{carb\text{-}sol}$ is small and constant. When the growth rate increases and gradually separates from equilibrium conditions, desolvation of the inner hydration sphere of aqueous Li^{+} ion increases the kinetic isotopic fractionation.

Note that the relationship between isotopes of divalent cations and growth rate can be expressed by the transition state theory (TST), assuming the generation of a $Ca_{1-x}Me_xCO_3$-composed diluted solid solution, whose rate of precipitation under steady-state chemical conditions is equivalent to that of the $CaCO_3$ phase. In fact, as shown in Fig. 2E, Fuger et al. (2022) managed to fit both published datasets using an adapted TST model, with specific backward calcite dissolution rate, distinguishing it from the one classically used for divalent ions. However, assuming that Li is a priori not present in calcite under a solid solution form, the same authors still consider desolvation as the most reasonable process explaining the observed negative trend.

2.5 Principal component analysis (PCA) of the combined effects

Overall, previous studies have shown that the inorganic calcite-solution Li isotopic fractionation appears little affected by temperature, salinity, and Li concentration of the growth solution, and display a higher influence of solution pH and kinetic effects related to the growth rate (see Fig. 2).

As the synergy of several parameters may control Li isotope fractionation and D(Li), we applied a principal component analysis (PCA) to the published inorganic calcite data in order to further identify the most influent parameters. In Fig. 3A, our principal component analysis was applied to the two experiments reporting growth rate data (Day et al., 2021; Füger et al., 2022). It indicates that the $\Delta^7Li_{carb\text{-}sol}$ and Log (Growth rate) anti-vary with each other on the principal component 1 (Dim 1), representing 69.4% of the whole dataset variability (other graphs and details on all Dimensions can be seen in the Supplementary Material). It overall shows that the variability between the two studies is discriminated primarily by $\Delta^7Li_{carb\text{-}sol}$ and Log(Growth rate), which is also consistent with Fig. 2E. Fig. 3A also highlights a strong relationship between D(Li) and Log(Growth rate) on Dim1. However, Day et al. data are grouped on this Dimension and therefore the growth rate does not participate much to their variance. On the other hand, the larger "intragroup" variability of the Fuger et al. data is mainly associated to pH variations following the principal component 2 (Dim 2), in agreement with Fig. 2D. Thus, this analysis shows that - based on the currently available data - the growth rate of calcite appears to be a major parameter for calcite Li isotope compositions.

Due the lack of growth rate data in Seyedali et al. (2021), we conducted another PCA, including other potentially relevant parameters that are available and also variable for the three considered experiments (e.g. bicarbonate ion concentration (HCO_3^-), carbonate ion concentration (CO_3^{2-}), calcium ion concentration (Ca^{2+}), solution pH, and the Saturation Index (SI)). Similarly, all details on all Dimensions are given in the

Sup. Mat. Even if there does not seem to be a dominant parameter in Dim1 explaining most of the variance, Fig. 3B shows that both $\Delta^7Li_{carb\text{-}sol}$ and D(Li) variability are mostly related to changes in solution pH and in dissolved Ca^{2+} concentrations. Since both parameters may influence the calcite growth rate, this result appears consistent with Fig. 2 CDEF.

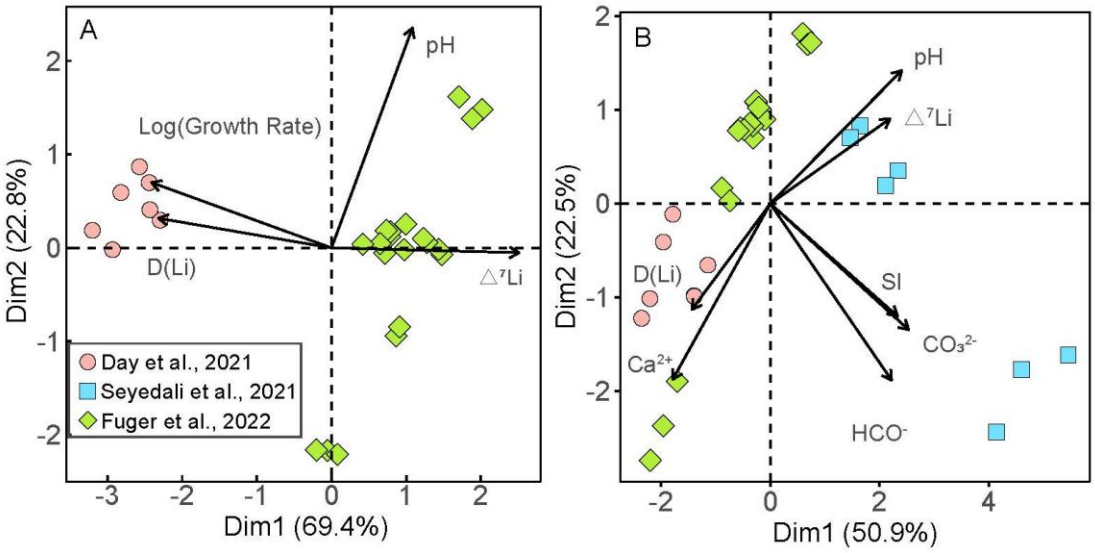

Fig. 3: Principal component analysis (PCA) for inorganically precipitated calcite. Dim 1 and Dim 2 are principal components 1 and 2. Arrow length is proportional to the percentage contribution of these first three principal components to the observed variation of each variable. **A)**, the relationship between D(Li), $\Delta^7Li_{carb\text{-}sol}$, pH, and the Log(Growth rate) is depicted. Dim 1, Dim 2 and Dim 3 represent 98.9% of the variability in the dataset. **B)** illustrates the relationship between $\Delta^7Li_{carb\text{-}sol}$, solution ions ($Ca^{2+}$, CO_3^{2-}, HCO_3^-), SI, and pH. Dim1, Dim2, and Dim3 explain 83.2% of the variability in the dataset. See Sup Mat for complementary PCA results (Fig. S1-1; S1-2).

The differences observed between the Seyedali et al, (2021) and the other two experiments can be distinguished in principal component 1, with HCO_3^-, CO_3^{2-} and SI contributing to the observed variations, which is consistent with experimental conditions (Table 2). On the other hand, the disparities within the Day et al., (2021) and the Fuger et al. (2022) datasets are mostly related to principal component 2, and

459 can be associated to differences in aqueous Ca^{2+} concentrations and pH. To some
460 extent, this may also be related to growth rates, at least for the Fuger et al. study,
461 which used Ca-based mass balance equations to determine them (see section 2.4).

462 3. Li/Ca and Li isotopes in biogenic carbonates

463 Several studies have been conducted to determine the role of environmental
464 parameters on Li/Ca ratios measured in biogenic carbonates. Field samples and
465 laboratory cultures demonstrate that the incorporation of Li is affected by a variety of
466 factors such as temperature, dissolved inorganic carbon (DIC), pH and biology ("vital
467 effects") (Dellinger et al., 2018; Hall and Chan, 2004; Hathorne et al., 2013; Lear and
468 Rosenthal, 2006; Roberts et al., 2018; Vigier et al., 2015). According to Delaney et al.
469 (1989), temperature initially appeared to significantly influence the Li/Ca ratio of
470 brachiopod shells, similar to that observed in synthetic calcite (Marriott et al., 2004).
471 However, no systematic relationship between Li/Ca and temperature has been found
472 for other types of biogenic carbonates. Instead, culture experiments and core top
473 studies have shown that the Li/Ca ratio of foraminifera is mostly influenced by
474 growth rate, solution Li/Ca ratio and DIC (Hall et al., 2005; Hathorne and James,
475 2006; Lear and Rosenthal, 2006; Vigier et al., 2015). Also for mollusks, Li/Ca ratios
476 have recently been inferred to result from a combination of biological processes,
477 growth rate, and planktic productivity (Dellinger et al., 2020; Thébault and Chauvaud,
478 2013; Thébault et al., 2009).

479 Concerning Li isotopes, it has been first considered that inorganic carbonate

precipitation experiments could provide a theoretical basis for the study of Li isotopic fractionation mechanism during carbonates growth. However, natural processes related to the organism biology may cause additional isotopic effects (Roberts et al., 2018; Dellinger et al., 2018; Vigier et al., 2015, Thibon et al., 2021). In particular, Li isotopes may be, at the cellular level, strongly fractionated during transmembrane active and passive transport (Poet, Vigier, Bouret et al., 2023). Some of these transporters (Na-H Exchangers: NHE) are ubiquist – present in all living species - and involved in intracellular pH regulation at play during the growth of calcifying species. In addition, different carbonate-producing organisms may form shells or skeletons with entirely different structures, growth rates, and mineralogy (Dellinger et al., 2018; Rollion-Bard et al., 2009). Besides, the calcifying fluid may be chemically and isotopically distinct from the seawater in which the organisms live. Another complication is that the environment in which organisms live may change over time (e.g., seawater pH, saturation state, nutrients). Finally, after the organism's death, sedimentary processes may bias the original carbonate isotopic signature, such as contamination by silicate minerals or Fe-Mn oxides, structure modification, isotope exchange, and fluid circulations during early diagenesis. In the following, we review the literature data (1) separating results from laboratory cultures and modern carbonates collected in the ocean and (2) providing a detailed focus on foraminifera data, since this group represents most of the published data, allowing statistical treatments. For this analysis, we took into account only the values validated by the authors as free from diagenetic effects, based on various geochemical tracers and/or

optical observations. Note that several methods have recently been developed for ensuring reliable and precise Li isotopic analyses of natural - low level - carbonate phases (e.g. Bastian et al., 2018; Pogge Von Strandmann et al., 2019; Van Hoecke et al., 2015).

3.1 Laboratory cultures of calcifying organisms: a means to study fractionating mechanisms

Several studies investigated "vital effects" on Li/Ca and Li isotopes through aquarium cultures of calcifying organisms, i.e. foraminifera (Roberts et al., 2018; Vigier et al., 2015), mollusks (Dellinger et al., 2018) and brachiopods (Gaspers et al., 2021). So far, all foraminifera cultured at the laboratory are calcitic and epi-benthic species (*Amphistegina lessonii* and *A. lobifera*), meaning that they operate photosynthesis and can thus be studied as a biological analogue to planktic species (Erez, 1978).

While inorganic carbonates $\Delta^7Li_{carb\text{-}sol}$ exhibit a positive correlation with pH (see Fig. 2C), this trend is not observed in foraminifera calcite grown in laboratory (Vigier et al. 2015) (*A. lobifera*). However, measurements were performed *in situ* by ion probe and the 0.7‰ variation expected for the studied pH range is challenging to reach with this method (Vigier et al. 2007). Roberts et al. (2018) cultivated *A. lessonni* and highlighted an opposite trend compared to the inorganic calcite, as for a pH increase from 7.9 to 8.6, a slight decrease in foraminifera δ^7Li was observed from 31.6‰ to 30.8‰ (measured using MC-ICP-MS, with a precision of ±0.4‰). Roberts et al.

523 (2018) suggested that a pH change induces the formation of another Li hydration
524 sphere (LiOH) in solution, which may increase the rates of ^{6}Li desolvation. However,
525 ion desolvation is usually related to the first hydration sphere and the formation of
526 LiOH is unlikely at this pH (Füger et al., 2022). The pH effect on calcifying
527 organisms and their Li isotopic composition therefore requires additional
528 investigations.
529 Vigier et al. (2015) showed that the $\delta^{7}Li$ values of cultured *A. lessonii* strongly depend
530 upon the seawater DIC concentrations, with foraminifera $\delta^{7}Li$ value ranging from
531 21.6‰ to 41.9‰ (measured by SIMS with a 2σ precision of ±2‰) for a DIC range of
532 1.0 to 3.0 mmol/kg. They suggested that Li^{+}, entering the cytoplasm through Na^{+}/H^{+}
533 exchanger (NHE), may fractionate Li isotopes in favor of the light ^{6}Li, as expected by
534 kinetic isotopic fractionation. A recent experimental study confirms the potential of
535 NHEs to strongly fractionate Li isotopes (Poet, Vigier, Bouret et al., 2023). Thus, a
536 low seawater DIC may lead to an increase in NHE activity in order to increase the pH
537 and the alkalinity of the calcifying fluid, promoting carbonate precipitation. This
538 process favours preferential ^{6}Li transfer. Unfortunately, Roberts et al. (2018) and
539 Vigier et al. (2015) did not report foraminifera growth rates, which is likely an
540 important factor influencing Li isotope composition (Roberts et al., 2018; Vigier et al.,
541 2015). For instance, an increase in seawater DIC may decrease the pH at the
542 foraminiferal surface (Glas et al., 2012), which may slow down the shell growth.
543 At high DIC (> 2 mmol kg^{-1}), Vigier et al. (2015) reported strong isotopic
544 fractionations in favor of the heavy ^{7}Li in *A. lessonni* tests ($\delta^{7}Li$ as high as 41.9‰).

545 Bivalve cultures also show positive biological Li isotopic fractionation in both their
546 shells and their soft tissues (see Dellinger et al., 2018; Thibon et al., 2021). A key role
547 of Li homeostasis has been inferred. When the internal balance of Li input and output
548 is disturbed by external conditions (e.g. high pH, high DIC, high Li contents), it is
549 expected that the isotope composition varies, because of NHE activity in particular.
550 The net internal Li budget can therefore be affected and may favor either the light or
551 the heavy isotope, depending on the ratio of input *versus* output fluxes (Thibon et al.,
552 2021).
553 The 3D graph shown in Fig. 4, may reconcile all foraminifera cultures data published
554 thus far. Indeed, there is a relationship between foraminifera δ^7Li and DIC when
555 foraminifera are cultured at a given and constant pH (red plane). At variable pH, when
556 the DIC is maintained constant, the foraminifera δ^7Li values remain constant (blue
557 plane, Vigier et al., 2015). In contrast, when both pH and DIC vary (Roberts et al.,
558 2018), Li isotopes follow a trend that cuts the previous datasets, indicating a
559 combination of both effects with a dominance of the pH effect (yellow line). Perhaps
560 compensating effects, related to intracellular H^+ and DIC homeostasis, may play a
561 major role in the Li transfer and resulting isotope compositions. Additional
562 experiments with variable pH at a much higher DIC could be useful to better
563 understand the Li isotope fractionation mechanisms at play in foraminifera cells.

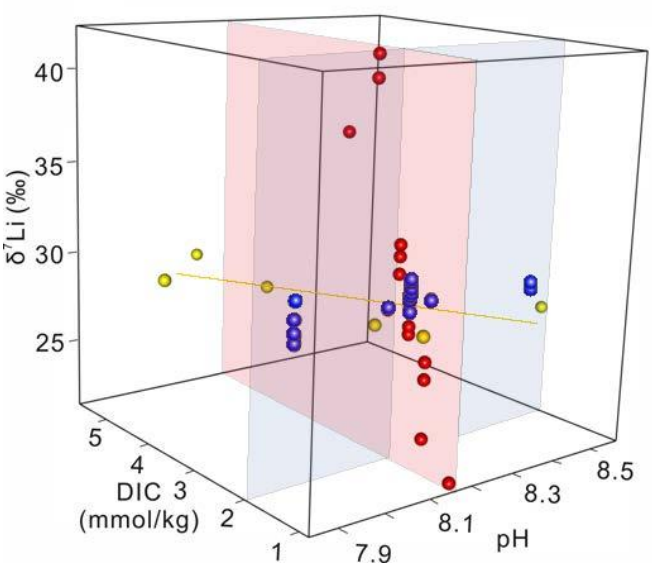

Fig. 4: Three-dimensional scatter plots of δ^7Li versus DIC and pH for cultured epi-benthic foraminifera. Blue plane indicates groups experiments performed at constant DIC. Red plane is for constant pH experiments (Vigier et al., 2015). The yellow dots show results obtained by Roberts et al. (2018) during an experiment where both DIC and pH varied.

Mollusks have also been cultured in laboratory-controlled conditions for investigating their shells Li compositions. Mollusk shells display Li/Ca ratios ranging from 7.1 to 25.3 µmol mol^{-1} and their δ^7Li values range from 17.2‰ to 39.6‰. Mollusk shell δ^7Li values are controlled by the mineral composition (aragonite *vs* calcite) and are only weakly related to the temperature (Dellinger et al., 2018). A significant amount of δ^7Li data for calcitic shells (*Mytilus edulis* and *Pecten maximus)* lie above the seawater isotopic composition, i.e. enriched in the heavy ^{7}Li (Dellinger et al., 2018), and cannot be explained by the sole effect of the growth rate. Dellinger et al. (2018) suggested that Li is actively removed from the calcification site, with an isotope fractionation in favour of the preferential removal of ^{6}Li. This hypothesis is supported by the negative correlation between δ^7Li and Li/Ca, as well as between δ^7Li and Mg/Ca, and are consistent with the key role of Li cell transporters (NHE) recently

582 highlighted at the cellular level (Poet, Vigier, Bouret et al., 2023).

583 Brachiopod culture experiments revealed that the Li concentration of calcitic
584 brachiopods (*Magellania venosa*) ranges from 2.3 to 3.5 ppm and their δ^7Li values
585 range from 27.5‰ to 28.1‰, with no significant effect of temperature (Gaspers et al.,
586 2021). In contrast, when pH decreases (from 7.6 to 7.35), there is a slight increase of
587 the Li isotopic fractionation, from -2.7‰ to -3.4‰, consistent with the trend
588 displayed by inorganic calcite. A higher solution $CaCl_2$ concentration (lower Mg/Ca
589 or Li/Ca ratios) also leads to a small increase in the Li isotope fractionation (from -2.7‰
590 to -4.6‰).

591 Overall, all laboratory cultures published thus far reveal that "vital effects" may
592 impact both Li concentrations and Li isotopic compositions of soft and calcified
593 tissues of foraminifera and mollusks.

594 3.2 Modern carbonates collected in the ocean

595 The environment of marine carbonates is more complex than that of in-lab synthesis
596 and aquarium cultures because it is more susceptible to disturbances by other
597 materials, such as contamination by marine particles (e.g., clays or Fe-Mn oxides), or
598 by processes occurring during early diagenesis or in the water column. However, the
599 study of modern marine shells is interesting because the Li isotopic composition of
600 the modern ocean is homogeneous, as well as its Li/Ca ratio, so the study of
601 contrasted isotopic signatures given by modern marine samples can give essential
602 clues. This however requires a good representative nature of the considered dataset.

603 According to the characteristics of the samples, published Li data can be divided into
604 two major categories. Several publications have sampled by picking various
605 organisms from the same species or from the same trophic group. This was performed
606 for foraminifera (Hall et al., 2005; Hathorne and James, 2006; Marriott et al., 2004;
607 Misra and Froelich, 2012; Roberts et al., 2018; Vigier et al., 2015), corals (Bastian et
608 al., 2018; Dellinger et al., 2020; Marriott et al., 2004; Misra and Froelich, 2009),
609 mollusks (Bastian et al., 2018; Dellinger et al., 2018), brachiopods (Washington et al.,
610 2020; Gaspers et al., 2021), and echinoderms (Dellinger et al., 2018). In most of these
611 studies, shells and tests are pre-cleaned in order to remove potential contamination
612 from oxides, silicate minerals or organic matter. In the second category of
613 publications, the whole carbonate fraction of a marine sediment sample was extracted
614 using a preferential dissolution by a weak acid generally (for modern carbonates:
615 Dellinger et al., 2020; Pogge Von Strandmann et al., 2019; for past reconstructions:
616 (Hall et al., 2005; Hathorne and James, 2006; Kalderon-Asael et al., 2021; Lechler et
617 al., 2015; Misra and Froelich, 2012; Murphy et al., 2022; Pogge Von Strandmann et
618 al., 2017; Pogge Von Strandmann et al., 2021; Pogge Von Strandmann et al., 2013;
619 Washington et al., 2020). In the following, the present study will refer to the
620 corresponding data as “bulk carbonates” (bulk). A couple of studies have compared
621 both methods (Bastian et al., 2018; Misra and Froelich, 2012; Pogge Von Strandmann
622 et al., 2019).
623 The current geographical distribution of all δ^7Li data published for marine carbonates
624 is shown in Fig. 5. This compilation includes biogenic carbonate samples primarily

from marine surface sediments (burial depths less than 2 cm), and for a small number, these data concern living organisms from the water column (e.g., foraminifera).

First of all, Fig 5 highlights significant gaps. Indeed, most studies (*viz*. 44% of the data) focus on the Atlantic Ocean, with a relatively small amount of data available for the Pacific Ocean, and only a few foraminifera data for the Indian Ocean. Another observation is that most studies concern the middle and low latitudes, and littoral environments. In the objective to use modern species as equivalent to reconstruct past variations of the open ocean Li isotopic composition - and its links with climate - these gaps appear essential to fill.

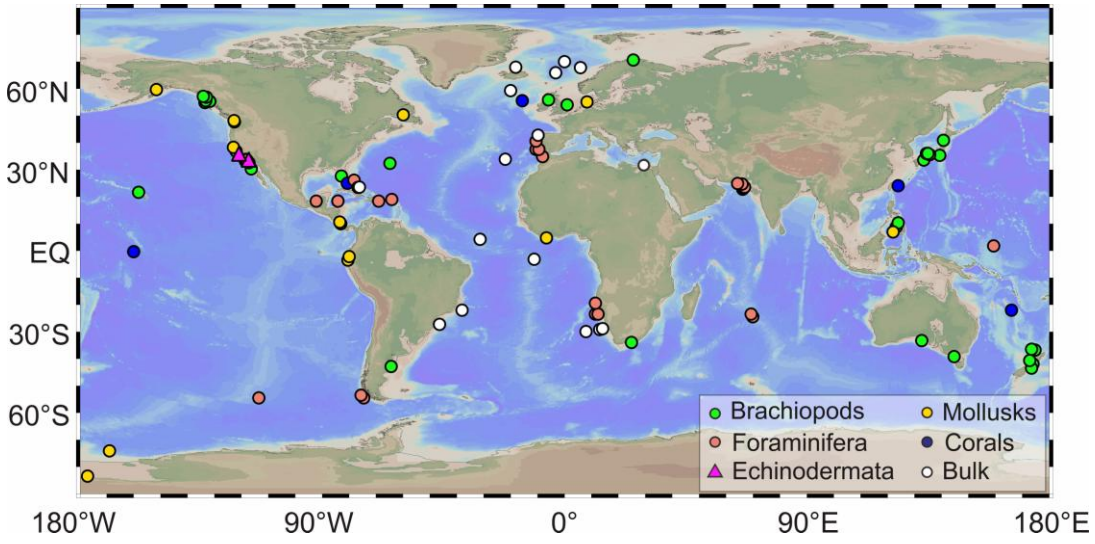

Fig. 5: Worldwide distribution of modern marine carbonates with published Li isotopic compositions. δ^7Li values concern corals (Bastian et al., 2018; Dellinger et al., 2020; Marriott et al., 2004; Misra and Froelich, 2009), foraminifera (Hall et al., 2005; Hathorne and James, 2006; Marriott et al., 2004; Misra and Froelich, 2012; Roberts et al., 2018; Vigier et al., 2015) mollusks (Bastian et al., 2018; Dellinger et al., 2018) brachiopods (Washington et al., 2020), echinoderms (Dellinger et al., 2018) and "bulk" carbonates (obtained by preferential dissolution, see text) (Bastian et al., 2018; Dellinger et al., 2020; Pogge Von Strandmann et al., 2019; Murphy et al., 2022).

644 It is possible to compare data among the different studied biological groups, keeping
645 in mind that all environmental conditions have not been explored similarly. This
646 allows us to highlight where the knowledge is the strongest and to evaluate the
647 representative nature of the average value that can be calculated for each one. As
648 shown in Fig. 6 and in Fig. S3, modern marine carbonates display a wide range of
649 δ^7Li values, from 14.9‰ (aragonitic mollusks, Dellinger et al. (2018)) to 40.7‰
650 (calcitic mollusks from Dellinger et al. (2018)). Marine calcite δ^7Li range from 19.5 ‰
651 to 40.7‰, high Mg calcite from 24.1‰ to 24.4‰ and aragonite from 14.9‰ to
652 23.8‰. There is a significant difference (Wilcoxon test: p-val. < 0.0001) between
653 aragonite (19.27 ± 3.7‰ n = 103) and calcite (28.14 ±6.5‰ n = 192) or high Mg
654 calcite (24.2 ± 0.3‰ n = 3). In contrast with laboratory precipitated inorganic
655 carbonates, which result in contrasting results, biogenic minerals highlight a more
656 systematic distinction between calcite and aragonite. Of note that there is a relatively
657 small statistical difference between calcite and high Mg calcite (Wilcoxon test: p-val.
658 < 0.01).
659 Among calcitic organisms, there are also significant differences (Wilcoxon test: p-val.
660 < 0.0001) between foraminifera (28.3 ± 5.9‰ n = 84), mollusks (30.9± 10.7‰ n =
661 33), and brachiopods (26.8 ± 1.8‰, n = 75), and they are all statistically higher than
662 bulk carbonates (i.e. extracted by preferential dissolution) (23.9 ± 2.1‰, n = 31). This
663 suggests that vital – biological - effects are able to influence the Li isotopic
664 composition of carbonates and that the Li isotopic fractionation can vary between
665 species and between individuals. Also, bulk - calcite - carbonate δ^7Li values are lower

than the data displayed by picked foraminifera, mollusks or brachiopods, indicating that there are still calcitic phases of importance (Foram ooze, Sponge spicules etc.), which have not been investigated yet, despite playing key role in the bulk fractions δ^7Li values.

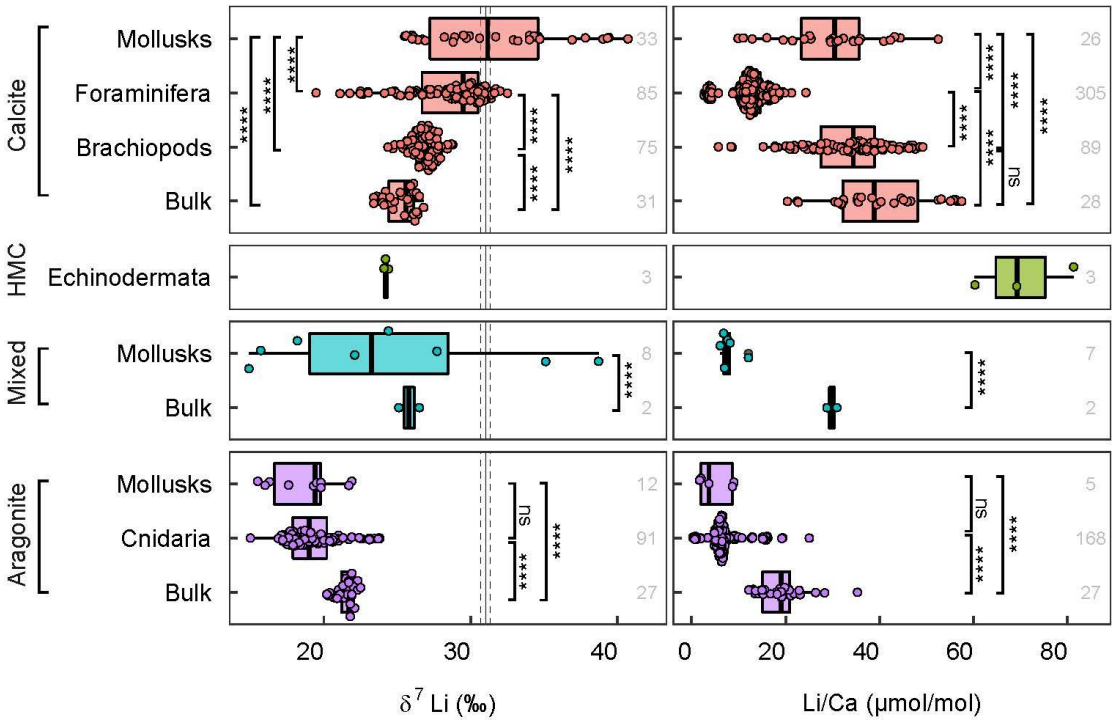

Fig. 6: Compilation of all existing data for δ^7Li and Li/Ca (in µmol mol-1) for modern (core top as circles, living as triangles) biogenic carbonates (Delaney et al., 1989; Hall and Chan, 2004; Marriott et al., 2004a; Marriott et al., 2004b; Hall et al., 2005; Yun et al., 2005; Hathorne and James, 2006; Vigier et al., 2007; Bryan and Marchitto, 2008; Hendry et al., 2009; Rollion-Bard et al., 2009; Misra and Froelich, 2012; Bastian et al., 2018; Roberts et al., 2018; Cuny-Guirriec et al., 2019; Pogge von Strandmann et al., 2019; Delinger et al., 2020; Washington et al., 2020; Gaspers et al., 2021; Dellinger et al., 2018). "HMC" denotes high magnesium calcite. "Mixed" denotes a mixture of calcite and aragonite. "Bulk" denotes sedimentary carbonate fraction extracted by preferential leaching (see text). The vertical solid and dashed line is for the seawater δ^7Li value (31 ± 0.3‰) (Millot et al., 2004). The seawater Li/Ca ratio is 2505 µmol mol^{-1}. Each data point represents a value for a carbonate sample. The grey numbers on the right denote the number of published data. Asterisks show the significance of the difference inferred through a Mann-Whitney-Wilcoxon tests: ns (not significant) for $p > 0.05$, * for $p < 0.05$, ** for $p < 0.01$, *** for $p < 0.001$, **** for $p < 0.0001$ (highly significant difference).

686

687 Among the aragonitic species, there is no significant difference in δ^7Li between corals
688 (19.4 ± 3.6‰, n = 91) and mollusks (18.2 ± 5.9‰, n = 12) ($p > 0.05$), but they are
689 both statistically different ($p < 0.0001$) from bulk carbonates (21.6 ± 1.3‰, n = 27).
690 In contrast with calcitic environments, the aragonitic bulk carbonate fractions display
691 higher δ^7Li values than all other groups studied thus far.

692 Most of the modern biogenic carbonates display lower δ^7Li values than seawater, such
693 as all brachiopods, echinodermata, and all aragonitic carbonates. However, some δ^7Li
694 values are higher than seawater, such as the calcitic shells of mollusks, and a small
695 fraction of foraminifera data. This indicates that they can be enriched in the heavier Li
696 isotope ^{7}Li relative to seawater, as observed in culture experiments (Vigier et al.,
697 2015). More recently, Thibon et al. (2021) showed that it is possible to have an
698 enrichment in ^{7}Li in marine soft tissues, depending on the Li input/output (excretion)
699 flux and of the magnitude of kinetic isotope fractionation related to the Li transport.

700 Concerning our compilation of Li/Ca ratios, it is striking that all modern marine
701 biogenic carbonates are significantly (by several orders of magnitude) depleted in Li
702 (<90 μmol mol^{-1}) compared to the present-day seawater value (2505 μmol mol^{-1}). On
703 average, calcite groups contain more Li than aragonite ones. By calculating the
704 LogD(Li) for these groups, we can compare their data to the ones found
705 experimentally for inorganic equivalents. In biogenic carbonates, LogD(Li) range
706 from -3.17 to -1.68, while they cover a wider range in inorganic phases, between
707 -5.70 and -1.99. Interestingly, for Li isotopes, the opposite is observed: the $\Delta^7Li_{carb\text{-}sol}$

distribution range for biogenic carbonates is larger than that for inorganic phases, independently of mineral types (see Fig. 1).

In biogenic calcite, Li/Ca ratios for mollusks, foraminifera, brachiopods, and bulk range from 9.9 to 52.5 μmol mol^{-1}, from 2.69 to 24.33 μmol mol^{-1}, from 5.7 to 49.2 μmol mol^{-1} and from 20.4 to 57.5 μmol mol^{-1}, respectively. Except for mollusks, there is a reverse trend between the average δ^7Li and the average Li/Ca ratio. In particular, foraminifera display the highest average isotopic composition and also the lowest Li/Ca ratio (12.48 ± 7.9 μmol mol^{-1}, n=305) (Fig. 6). Their range in Li/Ca ratios also appears restricted compared to the variations observed within each of the other groups. This may be due to the fact that Li/Ca ratios have been mostly measured in similar samples for which Li isotopes could be measured too. When no isotopic measurements were performed due to low Li levels, no Li concentration was measured neither and this limitation may induce a significant bias.

In contrast to biogenic calcite, biogenic aragonite appears to display a positive relationship between δ^7Li and Li/Ca, when comparing average values for mollusks, cnidarian, and bulk carbonates. Aragonitic mollusks are particularly depleted in Li compared to calcitic mollusks, although the number of data is small (Li/Ca = 5.02 ± 7.2 μmol mol^{-1}, n = 5). Cnidarians display relatively low Li/Ca ratios (7.33 ± 6.3 μmol mol^{-1}, n = 168), while bulk aragonite extracted from sedimentary fractions display the highest average Li/Ca ratio.

Finally, high-Mg calcite echinoderm specimens display the highest Li/Ca values of the whole carbonate dataset, although only 3 data are reported in the literature (70.27

730 ± 21.08 μmol mol^{-1}, n = 3) (Dellinger et al., 2018).

731 3.3 Focus on foraminifera species

732 Foraminifera are single-celled eukaryotic organisms belonging to the Phylum
733 *Granuloreticulosa* (Pearson, 2012), and many secrete a test (or shell) made of calcium
734 carbonate, generally low-Mg calcite, but possibly high-Mg calcite in porcelaneous
735 species, and aragonite in some groups. Some species may include sedimentary
736 particles (Pearson, 2012; Vigier et al., 2007). "Benthic" marine foraminifera majority
737 live on or within the seafloor sediment, while a number float in the water column at
738 various depths (known as "planktic") (Hemleben et al., 2012). Currently, studies of Li
739 isotopes in modern marine foraminifera are mainly focused on planktic species, while
740 relatively few studies have been conducted on natural benthic foraminifera species
741 (Table 3).

742 Planktic and benthic foraminifera do not exhibit significant differences in Li/Ca ratios,
743 except for the Antarctic Ocean where the Li/Ca ratio of planktic foraminifera is
744 statistically higher than that of benthic species (Table 3). In contrast, differences can
745 be observed for Li isotopes. At first, the Li isotopic compositions of living
746 foraminifera from the Pacific Ocean water column appear consistent with that of
747 foraminifera picked from surface sediments. This suggests that the Li isotopic signal
748 is not rapidly affected by early diagenesis (although specific chemical treatment
749 targeted the removal of contaminant phases and only data validated by authors as free
750 from diagenetic effects were considered).

751 Consequently, we included both living and sediments top-layer foraminifera in our
752 compilation. δ^7Li values vary from 24.9‰ to 32.5‰ for planktic foraminifera, and
753 from 19.4‰ to 27.3‰ for benthic ones (Fig. 7). There are significant differences
754 between planktic (29.7 ± 2.9‰ n=70) and benthic foraminifera (24 ± 4.1‰ n=23) (see
755 Table 4 and also Fig. S3).
756

757 Table 3 Compilation of δ^7Li and Li/Ca ratios measured for modern foraminifera (uncertainties are given at the standard deviation σ level)

Species	Source	Habits	n	δ^7Li (‰)	n	Li/Ca (μmol mol^{-1})	Reference
Orbulina universa	Living	Planktic	5	30.5 ± 0.3	5	11.32 ± 0.75	Misra and Froelich, 2012
Globigerina ruber	Coretop	Planktic	2	30.6 ± 0.1	2	13.51 ± 0.78	Misra and Froelich, 2012
Globigerina triloba	Coretop	Planktic	6	30.1 ± 0.6	6	12.88 ± 1.32	Misra and Froelich, 2012
Globigerinoides conglobatus	Coretop	Planktic	3	29.1 ± 0.8	3	10.92 ± 0.69	Misra and Froelich, 2012; Hathorne et al., 2006
Globigerinoides sacculifer	Coretop	Planktic	5	29.0 ± 0.6	14	12.34 ± 0.54	Hall et al., 2005; Misra and Froelich, 2012; Hathorne et al., 2006; Hall and Chan, 2004
Globorotalia cultrata	Coretop	Planktic	2	29.7 ± 0.2	2	11.90 ± 0.28	Hathorne et al., 2006
Globorotalia menardiib	Coretop	Planktic	1	29.1	1	12.50	Hall et al., 2005
Globorotalia merdii	Coretop	Planktic	4	30.2 ± 0.2	4	10.94 ± 1.14	Misra and Froelich, 2012
Globorotalia truncatulinoides	Coretop	Planktic	5	28.7 ± 1.5	3	12.97 ± 0.9	Hall et al., 2005; Hathorne et al., 2006 Vigier et al., 2007 Misra and Froelich, 2012
Globorotalia tumida	Coretop	Planktic	3	28.1 ± 1.5	3	11.56 ± 0.46	Hathorne et al., 2006 Misra and Froelich, 2012
Neogloboquadrina dutertrei	Coretop	Planktic	4	29.1 ± 0.8	4	12.73 ± 0.6	Hathorne et al., 2006 Misra and Froelich, 2012
Neogloboquadrina pachyderma	Coretop	Planktic			13	18.28 ± 0.70	Hendry et al., 2009
Orbulina universa	Coretop	Planktic	17	30.4 ± 0.8	32	11.9 ± 1.43	Hall et al., 2005; Hathorne et al., 2006 Misra and Froelich, 2012; Hall and Chan, 2004
Cibicidoides cicatricosus	Coretop	Benthic			5	15.36 ± 0.86	Hall and Chan, 2004
Cibicidoides incrassatus	Coretop	Benthic			7	14.47 ± 0.53	Hall and Chan, 2004
Cibicidoides mundulus	Coretop	Benthic	11	23.9 ± 1.8	11	13.08 ± 0.88	Roberts et al., 2018
Cibicidoides pachyderma	Coretop	Benthic			56	12.76 ± 1.44	Hall and Chan, 2004 ; Bryan and Marchitto, 2008
Cibicidoides robertsonianus	Coretop	Benthic			5	13.63 ± 0.81	Hall and Chan, 2004
Cibicidoides wuellerstorfi	Coretop	Benthic	7	23.6 ± 2.4	14	14.96 ± 2.23	Roberts et al., 2018; Hall and Chan, 2004 2005 Yun
Cibicidoides rugosus	Coretop	Benthic			5	14.22 ± 0.49	Hall and Chan, 2004
Euuvigerina sp.	Coretop	Benthic	1	21.1	1	14.4	Marriott et al., 2004a
Hoeglundina elegans	Coretop	Benthic			37	3.78 ± 0.50	Bryan and Marchitto, 2008
Planulina ariminensis	Coretop	Benthic			17	13.76 ± 1.45	Bryan and Marchitto, 2008
Planulina foveolata	Coretop	Benthic			13	12.31 ± 1.41	Bryan and Marchitto, 2008
Uvigerina peregrina	Coretop	Benthic			36	16.70 ±1 .90	Bryan and Marchitto, 2008

Uvigerina sp.	Coretop	Benthic	3	25.8 ± 0.8	3	17.53 ±1.34	Marriott et al., 2004a	

758

In contrast, we detect no significant difference between the different oceans for either planktic or benthic foraminifera, but the number of data is small and the test power would deserve to be reinforced with additional data for Pacific and Indian oceans.

Table 4. Average δ^7Li and Li/Ca values for modern foraminifera from different oceans and habitats (uncertainties are standard deviation (SD))

	n	δ^7Li (‰)	n	Li/Ca (μmol mol^{-1})
Living	**5**	**30.5 ± 0.3**	**5**	**11.32 ± 0.75**
Planktic	**5**	**30.5 ± 0.3**	**5**	**11.32 ± 0.75**
Pacific ocean	5	30.5 ± 0.3	5	11.32 ± 0.75
Coretop	**78**	**28.1 ± 3.0**	**299**	**12.48 ± 3.98**
Planktic	**56**	**29.7 ± 1.1**	**89**	**12.86 ± 2.57**
Antarctic			13	18.28 ± 0.70
Atlantic	44	29.6 ± 1.2	75	11.94 ± 1.30
Indian ocean	7	29.8 ± 0.8		
Pacific ocean	5	30.1 ± 1.2	1	11.50
Benthic	**22**	**24.0 ± 2.0**	**210**	**12.32 ± 4.44**
Atlantic	14	23.4 ± 1.9	203	12.24 ± 4.46
Indian ocean	4	24.6 ± 2.4	4	16.75 ± 1.91
Pacific ocean	4	25.3 ± 1.7	3	12.07 ± 0.90

If representative, the published dataset would indicate that foraminifera δ^7Li values do not differ significantly among the different oceans, in the horizontal direction, while in the vertical direction, planktic and benthic habitats play a more decisive role in the foraminifera Li isotopic composition. The higher δ^7Li values measured systematically in planktic species (compared to the benthic ones collected in the same ocean) are consistent with a pH control. Indeed, in modern oceans, the pH of surface seawater (up to 8.33 ± 0.1) is usually higher than that of the bottom seawater (down to 7.52 ± 0.05) (Lauvset et al., 2020), except close to hydrothermal sites. Indeed, there is a

positive correlation between pH and $\Delta^7Li_{carb\text{-}sol}$ observed in inorganic calcite (Fig. 2C) (Füger et al., 2022; Seyedali et al., 2021), i.e. with no influence of biology. However, the large difference observed between the two marine habitats (benthic and planktic) cannot be explained by the slope shown in Fig. 2C. Indeed, the published sampling depth of benthic foraminifera is considerable, ranging from 96 to 3729 m (Marriott et al., 2004; Roberts et al., 2018), which corresponds to a pH range as large as for the whole seawater one. Thus, substituting the highest (8.33) and lowest (7.52) seawater pH into the equation in Fig. 2C, yields isotopic fractionations ($\Delta^7Li_{carb\text{-}sol}$) of -3.2‰ and -4.2‰, respectively, so the theoretical maximum isotopic difference that can be produced between planktic and benthic (using the regression shown in Fig. 2C) is 1‰. In contrast, benthic foraminifera δ^7Li values are lower by -6 or -7‰ from the seawater value while planktic δ^7Li are lower by -1 to -3‰. Consequently, other factors such as biological processes, growth rates and temperature would deserve to be investigated in the future.

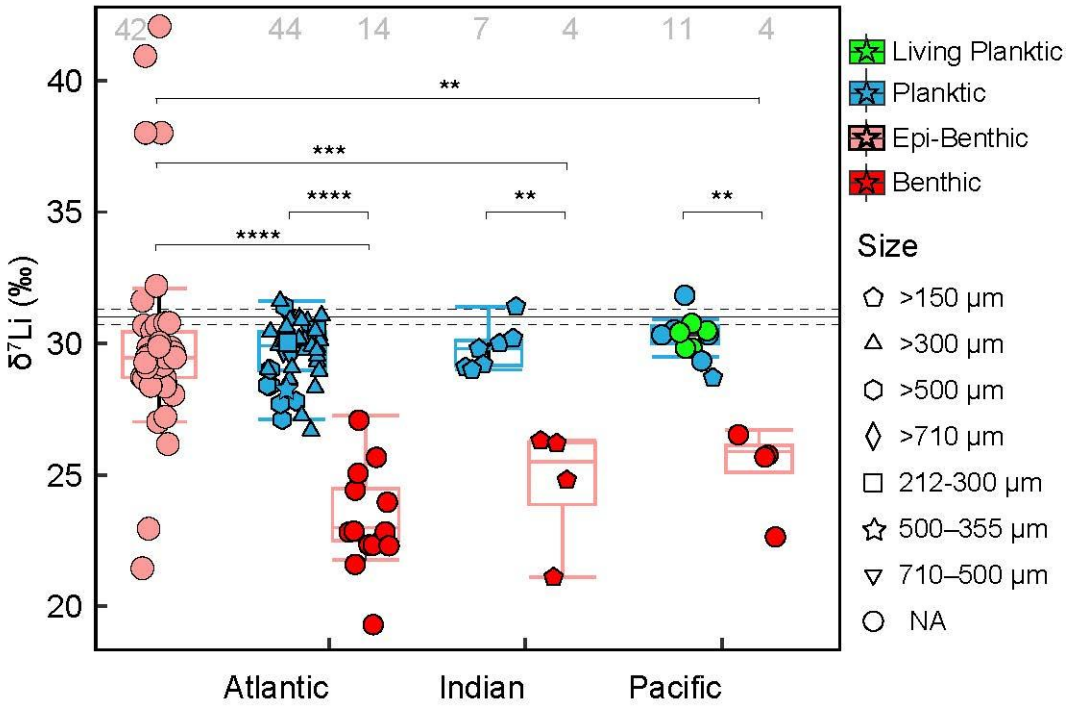

787

788 **Fig. 7:** The Li isotopic composition of modern oceanic foraminifera of different habitats
789 distinguished by oceans, except epi-benthic foraminifera, coming from laboratory-cultured (in
790 pink). The horizontal bars represent the seawater line. Asterisks show the significance of the
791 Mann-Whitney-Wilcoxon tests used to observe differences between pairs of groups: ns (not
792 significant) for $p > 0.05$, * for $p < 0.05$, ** for $p < 0.01$, *** for $p < 0.001$, **** for $p <$
793 0.0001 (highly significant difference).

794 Interestingly, we found a negative linear correlation between the δ^7Li and Li/Mg ratio
795 for benthic and planktic foraminifera (Fig. 9). Li/Mg ratio of corals and foraminifera
796 is more strongly related to temperature than Li/Ca, and has been recently proposed as
797 a proxy for reconstructing global ocean temperature (Rollion-Bard and Blamart, 2015;
798 Stewart et al., 2020; Zhu et al., 2021). Although this temperature indicator is mostly
799 applied to aragonitic carbonates and high-Mg calcite thus far, a similar correlation can
800 be observed for the calcitic foraminifera dataset (Fig. 9). Therefore, we cannot
801 completely rule out that differences in seawater surface and bottom temperatures may

lead to the formation of different Li/Mg ratios in planktic and benthic foraminifera, which in turn result in differences in their Li isotopic compositions.

The growth rate may also be an additional factor affecting the Li isotopic composition of calcite, as shown in Fig. 2E for inorganic phases, where low growth rate corresponds to higher calcite δ^7Li (within the range of ocean pH). However, it is more complicated for foraminifera, as their growth rate may also be a function of metabolism, nutrient availability and environmental conditions. Due to the lack of published data of foraminifera growth rates coupled with Li measurements, we cannot further explore the influence of this factor to explain the observed difference between planktic and benthic species.

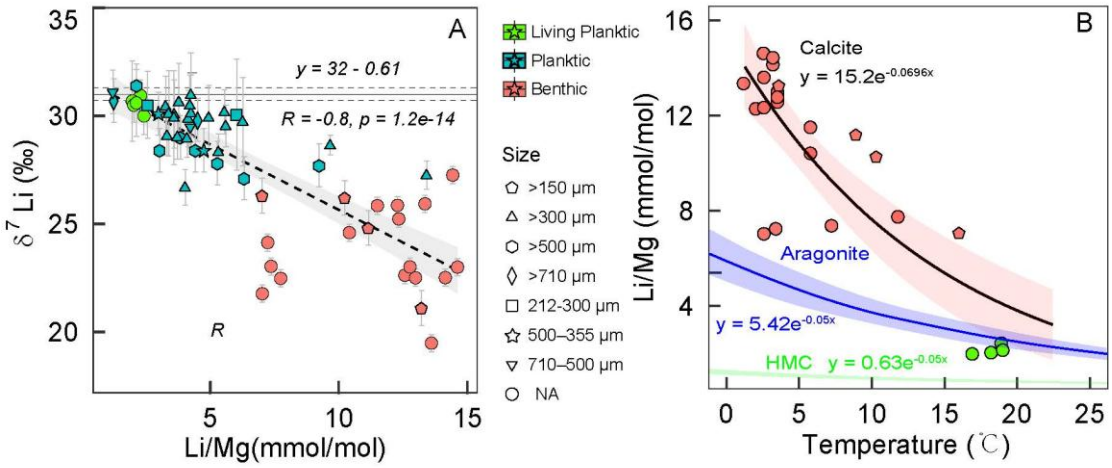

Fig. 8: A) Li isotopic composition of modern foraminifera versus Li/Mg ratio measured in their shells; and **B)** Li/Mg versus seawater temperature. Each data point represents a carbonate sample. The black line with pink shade is the regression of compilation data for foraminifera. The blue solid lines report previous aragonitic phases data regression (Stewart et al., 2020), and bright green solid lines reports HMC data regression (Stewart et al., 2020). Shadings show 95% confidence intervals.

821 Due to the lack of published data of foraminifera growth rates coupled with Li
822 measurements, we cannot further explore the influence of this factor to explain the
823 observed difference between planktic and benthic species.
824 Based on our compilation (Table 3), it is however possible to evaluate the "species
825 effect", by quantifying the significance of isotopic differences between various genera
826 of planktic foraminifera (Fig. 9). The δ^7Li values of *Globigerinoides* (28.8 ± 1.9‰, n
827 = 9) are statistically lower ($p < 0.001$) than those of *Globigerina* (30.2 ± 1.1‰ n = 8)
828 and *Orbulina* (30.5 ± 1.6‰ n = 25). Statistical differences ($p < 0.01$) are also
829 observed between *Orbulina* (30.5 ± 1.6‰ n = 25) and *Neogloboquadrina* (28.2 ± 2.9‰
830 n=5). It should be noted that the number of *Globigerinoides* (9)， *Globigerina* (8) *and*
831 *Neogloboquadrina* (5) samples is relatively small. No significant difference are
832 revealed between living *Orbulina universa* (30.6 ± 0.62‰ n=6) and core-top
833 *Orbulina universa* (30.5 ± 1.8‰， n=19), confirming the lack of impact of rapid
834 diagenesis, at least for this species (or correct pre-cleaning conditions as inferred
835 previously).
836 Concerning Li/Ca ratio, Fig. 9 shows no "species effect" for planktic foraminifera,
837 while this ratio is much more variable among benthic species. However, as described
838 in section 2, this observation may be biased by the lack of Li concentrations
839 measurements made in foraminifera tests not providing enough material for Li isotope
840 measurements. This may concern low Li level species, low density (e.g. porous, thin)
841 tests, or species with a weak abundancy in the sediment.

We investigated the role of the size fractions in the isotopic and chemical differences observed between foraminifera species or habitats. However, in many publications, the precise determination of this parameter is not provided, with access often limited to either a broad range of sizes or only the minimum size. As depicted in Fig. S4 and Fig. S5, no significant relationship with size can be observed at this stage. It is noteworthy that the 2D size fraction of foraminifera may not be directly linked to the growth rate, as it is influenced by factors such as the carbonate structure and density, lifespan, and other biological processes involved in the biomineralization process.

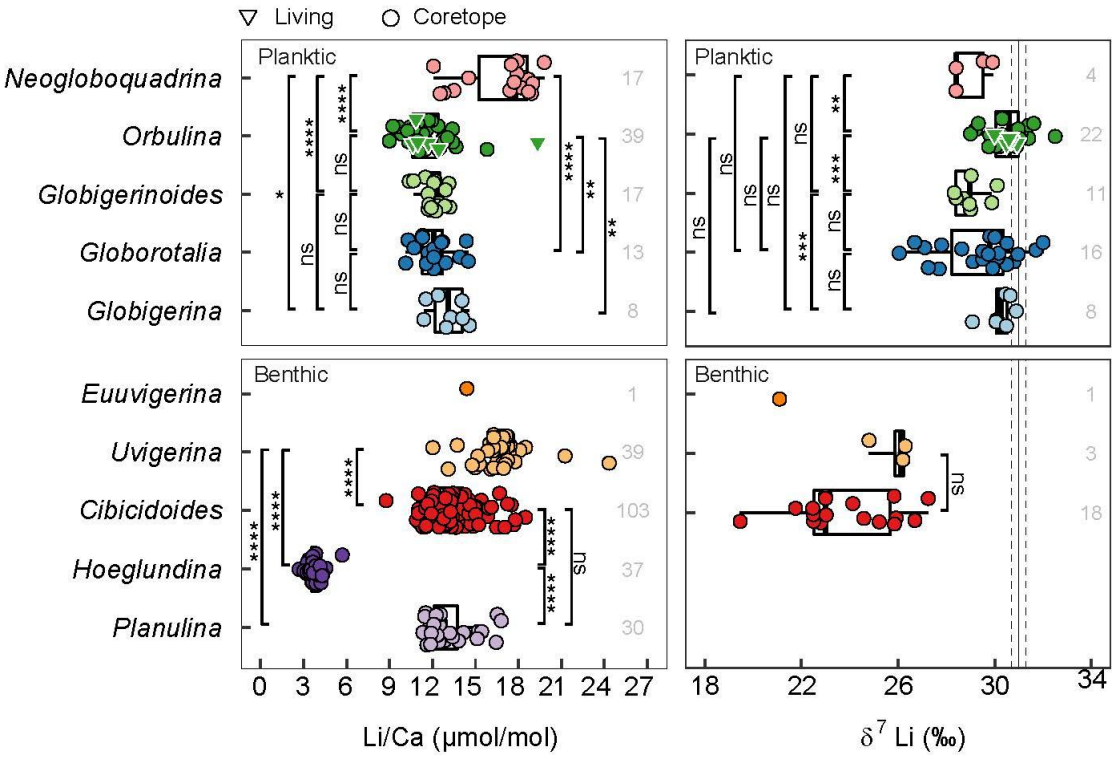

Fig. 9: Box plots exhibiting Li/Ca ratios and Li isotope compositions of modern foraminifera, organized by phylum. Seawater δ^7Li are added as a grey bar for comparison. The numbers at the right of each box indicate the number of samples. Asterisks show the significance of the Mann-Whitney-Wilcoxon tests used to observe differences between pairs of groups: ns (not significant) for $p > 0.05$, * for $p < 0.05$, ** for $p < 0.01$, *** for $p < 0.001$, **** for $p < 0.0001$ (highly significant difference). For a representation with size fractions included, see

857 Fig. S4.

858 ## 4. Conclusions

859 This review compiled and investigated major studies of Li/Ca and Li isotopes in
860 inorganic and biogenic carbonates, providing an overview of the actual state of
861 knowledge in the field. It primarily shows that it is extremely difficult to highlight
862 "vital effects" - or the lack of "vital effects" – simply by using a direct comparison
863 between biogenic and inorganic carbonates. Indeed, both types of carbonates vary
864 significantly - and generally differently - as a function of specific parameters. Another
865 point of attention is the various gaps in the knowledge concerning the influence of
866 mineral types, growth rates, environmental conditions outside the Atlantic Ocean, and
867 calcifying species with low Li/Ca ratios. Finally, we highlighted that the combination
868 of Li/Ca and Li isotopes appear to be useful for interpreting the influence of
869 environmental or biological parameters. In more detail, we observed the following
870 main points:

871 **For inorganic carbonates:**

872 - Current experimental studies mainly focused on calcite, while relatively little data
873 are available for aragonite and high-Mg calcite. It is therefore too early to
874 determine the role of the carbonate structure and mineralogy on Li isotopes.
875 - The temperature has little to no effect on the Li isotopic composition of inorganic
876 calcite, but changes in temperature can affect calcite Li/Ca ratios.
877 - The extent of Li isotope fractionation between calcite and solution can be

878 significantly affected by solution pH. More ^{6}Li is incorporated into calcite at low
879 pH. The recently inferred explanation is that there is a Li speciation effect at the
880 mineral surface.

881 - A similar situation arises for growth rate: an increase in calcite growth rate leads
882 to an increase in D(Li) values and in the Li isotope fractionation. The
883 interpretation is still debated.

884 **For biogenic carbonates:**

885 - Marine biogenic carbonate studies mainly concern the Atlantic Ocean (44% of
886 the data), so more effort should be put into other oceanic conditions in order to
887 cover a broader range of environmental conditions.

888 - $\delta^{7}Li$ values are statistically different between foraminifera, mollusks, and
889 brachiopods, and they are all statistically higher than the values measured in bulk
890 carbonates. This strongly suggests that vital - biological - effects can influence
891 the Li isotopic composition of biogenic carbonates and that the isotopic
892 fractionation of Li isotopes can vary between species and between individuals.

893 - The $\delta^{7}Li$ values of planktic foraminifera are statistically higher than those of
894 benthic foraminifera. Statistical differences are also evidenced between different
895 species of planktic foraminifera. This supports a key role of genetics and
896 metabolic effects that may be explored for future paleo reconstructions. In
897 particular, the relationship between foraminiferal Li/Mg ratio and temperature
898 suggests a new potential for reconstructing paleo-temperature that would deserve
899 to be reinforced.

Acknowledgements

Dongyu Chen was supported by a China Scholarship Council funding that we acknowledge (CSC NO. 202006260006) for his three years PhD study at the Laboratory of Oceanography of Villefranche in France (LOV). Authors also acknowledge financial support from the ANR ISO2MET (//anr.fr/Projet-ANR-18-CE34-514 0002; www.iso2met-project.fr/). On behalf of M.M., the IAEA is grateful to the Government of the Principality of Monaco for the support provided to its Marine Environment Laboratories. Finally, we greatly thank the three reviewers and the editor for their fruitful and detailed comments that helped improving the manuscript.

References

Artigue, L., Chavagnac, V., Destrigneville, C., Ferron, B. and Cathalot, C., 2022. Tracking the Lithium and Strontium Isotope Signature of Hydrothermal Plume in the Water Column: A Case Study at the EMSO-Azores Deep-Sea Observatory. Frontiers in Environmental Chemistry, 3.

Bastian, L. et al., 2018. Lithium Isotope Composition of Marine Biogenic Carbonates and Related Reference Materials. Geostandards and Geoanalytical Research, 42(3): 403-415.

Busenberg, E. and Niel Plummer, L., 1985. Kinetic and thermodynamic factors controlling the distribution of $SO_3^{2-}$and Na^+ in calcites and selected aragonites. Geochimica et Cosmochimica Acta, 49(3): 713-725.

Chan, L., Edmond, J.M. and Thompson, G., 1993. A lithium isotope study of hot springs and metabasalts from mid-ocean ridge hydrothermal systems. Journal of Geophysical Research, 98(B6): 9653-9659.

Chan, L., Gieskes, J.M., You, C. and Edmond, J.M., 1994. Lithium isotope geochemistry of sediments and hydrothermal fluids of the Guaymas Basin, Gulf of California. Geochimica et cosmochimica acta, 58(20): 4443-4454.

Day, C.C., Pogge Von Strandmann, P.A.E. and Mason, A.J., 2021. Lithium isotopes and partition coefficients in inorganic carbonates: Proxy calibration for weathering reconstruction. Geochimica et Cosmochimica Acta, 305: 243-262.

Delaney, M.L., Popp, B.N., Lepzelter, C.G. and Anderson, T.F., 1989. Lithium-to-calcium ratios in modern, Cenozoic, and Paleozoic articulate brachiopod shells. Paleoceanography, 4(6): 681-691.

Dellinger, M. et al., 2015. Riverine Li isotope fractionation in the Amazon River basin controlled by the weathering regimes. Geochimica et Cosmochimica Acta, 164: 71-93.

Dellinger, M. et al., 2018. The Li isotope composition of marine biogenic carbonates: Patterns and mechanisms. Geochimica et Cosmochimica Acta, 236: 315-335.

Dellinger, M. et al., 2020. The effects of diagenesis on lithium isotope ratios of shallow marine carbonates. American Journal of Science, 320(2): 150-184.

Erez, J., 1978. Vital effect on stable-isotope composition seen in foraminifera and coral skeletons. Nature (273): 199-202.

Foster, G.L. and Rae, J.W.B., 2016. Reconstructing Ocean pH with Boron Isotopes in Foraminifera. Annual Review of Earth and Planetary Sciences, 44(1): 207-237.

Füger, A. et al., 2022. Effect of growth rate and pH on Li isotope fractionation during its incorporation in calcite. Geochimica et Cosmochimica Acta, 323: 276-290.

Füger, A., Konrad, F., Leis, A., Dietzel, M. and Mavromatis, V., 2019. Effect of growth rate and pH on lithium incorporation in calcite. Geochimica et cosmochimica acta, 248: 14-24.

Gabitov, R. et al., 2019. Elemental uptake by calcite slowly grown from seawater solution: An in-situ study via depth profiling. Frontiers in Earth Science, 7.

Gabitov, R.I. et al., 2011. In situ δ^7Li, Li/Ca, and Mg/Ca analyses of synthetic aragonites. Geochemistry, Geophysics, Geosystems, 12(3).

Gabitov, R.I. and Watson, E.B., 2006. Partitioning of strontium between calcite and fluid. Geochemistry, Geophysics, Geosystems, 7(11).

Gaspers, N. et al., 2021. Lithium elemental and isotope systematics of modern and cultured brachiopods: Implications for seawater evolution. Chemical Geology, 586: 120566.

Glas, M.S., Fabricius, K.E., de Beer, D., Uthicke, S. and Gilbert, J.A., 2012. The O_2, pH and Ca_{2+} microenvironment of benthic foraminifera in a high CO_2 world. PloS one, 7(11): e50010-e50010.

Hall, J.M. and Chan, L., 2004. Li/Ca in multiple species of benthic and planktic foraminifera: Thermocline, latitudinal, and glacial – interglacial variation. Geochimica et Cosmochimica Acta, 68(3): 529–545.

Hall, J.M., Chan, L.H., McDonough, W.F. and Turekian, K.K., 2005. Determination of the lithium isotopic composition of planktic foraminifera and its application as a paleo-seawater proxy. Marine Geology, 217(3-4): 255-265.

Hathorne, E.C. and James, R.H., 2006. Temporal record of lithium in seawater: A tracer for silicate weathering? Earth and Planetary Science Letters, 246(3-4): 393-406.

Hathorne, E.C., Felis, T., Suzuki, A., Kawahata, H. and Cabioch, G., 2013. Lithium in the aragonite skeletons of massivePorites corals: A new tool to reconstruct tropical sea surface temperatures. Paleoceanography, 28(1): 143-152.

Huh, Y., Chan, L., Zhang, L. and Edmond, J.M., 1998. Lithium and its isotopes in major world rivers; implications for weathering and the oceanic budget. Geochimica et cosmochimica acta, 62(12): 2039-2051.

Kalderon-Asael, B. et al., 2021. A lithium-isotope perspective on the evolution of carbon and silicon cycles. Nature, 595(7867): 394-398.

Lauvset, S.K. et al., 2020. Processes Driving Global Interior Ocean pH Distribution. Global Biogeochemical Cycles, 34(1).

Lear, C.H. and Rosenthal, Y., 2006. Benthic foraminiferal Li/Ca; insights into Cenozoic seawater carbonate saturation state. Geology (Boulder), 34(11): 985-988.

Lechler, M., Pogge Von Strandmann, P.A.E., Jenkyns, H.C., Prosser, G. and Parente, M., 2015. Lithium-isotope evidence for enhanced silicate weathering during OAE 1a (Early Aptian Selli event). Earth and Planetary Science Letters, 432: 210-222.

Marriott, C.S., Henderson, G.M., Belshaw, N.S. and Tudhope, A.W., 2004. Temperature dependence of δ^7Li, δ^{44}Ca and Li/Ca during growth of calcium carbonate. Earth and Planetary Science Letters, 222(2): 615-624.

Marriott, C.S., Henderson, G.M., Crompton, R., Staubwasser, M. and Shaw, S., 2004. Effect of mineralogy, salinity, and temperature on Li/Ca and Li isotope composition of calcium carbonate. Chemical Geology, 212(1): 5-15.

Mavromatis, V. et al., 2018. Barium partitioning in calcite and aragonite as a function of growth rate. Geochimica et Cosmochimica Acta, 237: 65-78.

Mavromatis, V., Gautier, Q., Bosc, O. and Schott, J., 2013. Kinetics of Mg partition and Mg stable isotope fractionation during its incorporation in calcite. Geochimica et Cosmochimica Acta, 114: 188-203.

Misra, S. and Froelich, P.N., 2012. Lithium Isotope History of Cenozoic Seawater:

Changes in Silicate Weathering and Reverse Weathering. Science, 335(6070): 818-823.

Murphy, J.G., Ahm, A.C., Swart, P.K. and Higgins, J.A., 2022. Reconstructing the lithium isotopic composition (δ^7Li) of seawater from shallow marine carbonate sediments. Geochimica et Cosmochimica Acta.

Okumura, M. and Kitano, Y., 1986. Coprecipitation of alkali metal ions with calcium carbonate. Geochimica et Cosmochimica Acta, 50(1): 49-58.

Olsher, U., Izatt, R.M., Bradshaw, J.S. and Dalley, N.K., 1991. Coordination chemistry of lithium ion: A crystal and molecular structure review. Chemical Reviews, 91(2).

Pearson, P.N., 2012. Oxygen Isotopes in Foraminifera: Overview and Historical Review. The Paleontological Society Papers, 18: 1-38.

Pierrot, D.E.L. and Wallace, D.W.R., 2006. MS Excel Program Developed for CO2 System Calculations. Carbon Dioxide Information Analysis Center, Oak Ridge National Laboratory.

Poet, M. et al., 2023. Biological fractionation of lithium isotopes by cellular Na(+)/H(+) exchangers unravels fundamental transport mechanisms. iScience, 26(6): 106887.

Pogge Von Strandmann, P.A.E. et al., 2017. Global climate stabilisation by chemical weathering during the Hirnantian glaciation. Geochemical Perspectives Letters: 230-237.

Pogge Von Strandmann, P.A.E. et al., 2019. Assessing bulk carbonates as archives for seawater Li isotope ratios. Chemical Geology, 530: 119338.

Pogge Von Strandmann, P.A.E. et al., 2021. Lithium isotope evidence for enhanced weathering and erosion during the Paleocene-Eocene Thermal Maximum. Science Advances, 7(42): eabh4224.

Pogge Von Strandmann, P.A.E., Jenkyns, H.C. and Woodfine, R.G., 2013. Lithium isotope evidence for enhanced weathering during Oceanic Anoxic Event 2. Nature Geoscience, 6(8): 668-672.

Roberts, J. et al., 2018. Lithium isotopic composition of benthic foraminifera: A new proxy for paleo-pH reconstruction. Geochimica et Cosmochimica Acta, 236: 336-350.

Rollion-Bard, C. et al., 2009. Effect of environmental conditions and skeletal ultrastructure on the Li isotopic composition of scleractinian corals. Earth and Planetary Science Letters, 286(1-2): 63-70.

Rollion-Bard, C. and Blamart, D., 2015. Possible controls on Li, Na, and Mg incorporation into aragonite coral skeletons. Chemical Geology, 396: 98-111.

Seyedali, M., Coogan, L.A. and Gillis, K.M., 2021. The effect of solution chemistry on elemental and isotopic fractionation of lithium during inorganic precipitation of calcite. Geochimica et Cosmochimica Acta, 311: 102-118.

Steinhoefel, G., Brantley, S.L. and Fantle, M.S., 2021. Lithium isotopic fractionation during weathering and erosion of shale. Geochimica et Cosmochimica Acta, 295: 155-177.

Stewart, J.A. et al., 2020. Refining trace metal temperature proxies in cold-water scleractinian and stylasterid corals. Earth and planetary science letters, 545: 116412.

Taylor, H.L., Duivestein, I.J.K., Farkas, J., Dietzel, M. and Dosseto, A., 2019. Technical note: Lithium isotopes in dolostone as a palaeo-environmental proxy – an experimental approach. Climate of the Past, 15(2): 635-646.

Thébault, J. and Chauvaud, L., 2013. Li/Ca enrichments in great scallop shells (Pecten maximus) and their relationship with phytoplankton blooms. Palaeogeography,

Palaeoclimatology, Palaeoecology, 373: 108-122.

Thébault, J., Schöne, B.R., Hallmann, N., Barth, M. and Nunn, E.V., 2009. Investigation of Li/Ca variations in aragonitic shells of the ocean quahog Arctica islandica, northeast Iceland. Geochemistry, Geophysics, Geosystems, 10(12).

Thibon, F. et al., 2021. Bioaccumulation of Lithium Isotopes in Mussel Soft Tissues and Implications for Coastal Environments. ACS Earth and Space Chemistry, 5(6): 1407-1417.

Thibon, F. et al., 2021. Large-scale survey of lithium concentrations in marine organisms. Science of The Total Environment, 751: 141453.

Van Hoecke, K. et al., 2015. Single-step chromatographic isolation of lithium from whole-rock carbonate and clay for isotopic analysis with multi-collector ICP-mass spectrometry. Journal of Analytical Atomic Spectrometry, 30(12): 2533-2540

Vigier, N., Rollion-Bard, C., Levenson, Y. and Erez, J., 2015. Lithium isotopes in foraminifera shells as a novel proxy for the ocean dissolved inorganic carbon (DIC). Comptes Rendus Geoscience, 347(1): 43-51.

Vigier, N., Rollion-Bard, C., Spezzaferri, S. and Brunet, F., 2007. In situ measurements of Li isotopes in foraminifera. Geochemistry, Geophysics, Geosystems, 8(1).

Washington, K.E. et al., 2020. Lithium isotope composition of modern and fossilized Cenozoic brachiopods. Geology, 48(11): 1058-1061.

Watson, E.B., 2004. A conceptual model for near-surface kinetic controls on the trace-element and stable isotope composition of abiogenic calcite crystals. Geochimica et Cosmochimica Acta, 68(7): 1473-1488.

Zhu, C., Chen, T. and Zhao, L., 2021. Magnesium partitioning into vaterite and its potential role as a precursor phase in foraminiferal Mg/Ca thermometer. Earth and Planetary Science Letters, 567: 116989.